Figures and figure supplements

Estrogen receptor alpha somatic mutations Y537S and D538G confer breast cancer endocrine resistance by stabilizing the activating function-2 binding conformation

Sean W Fanning *et al*

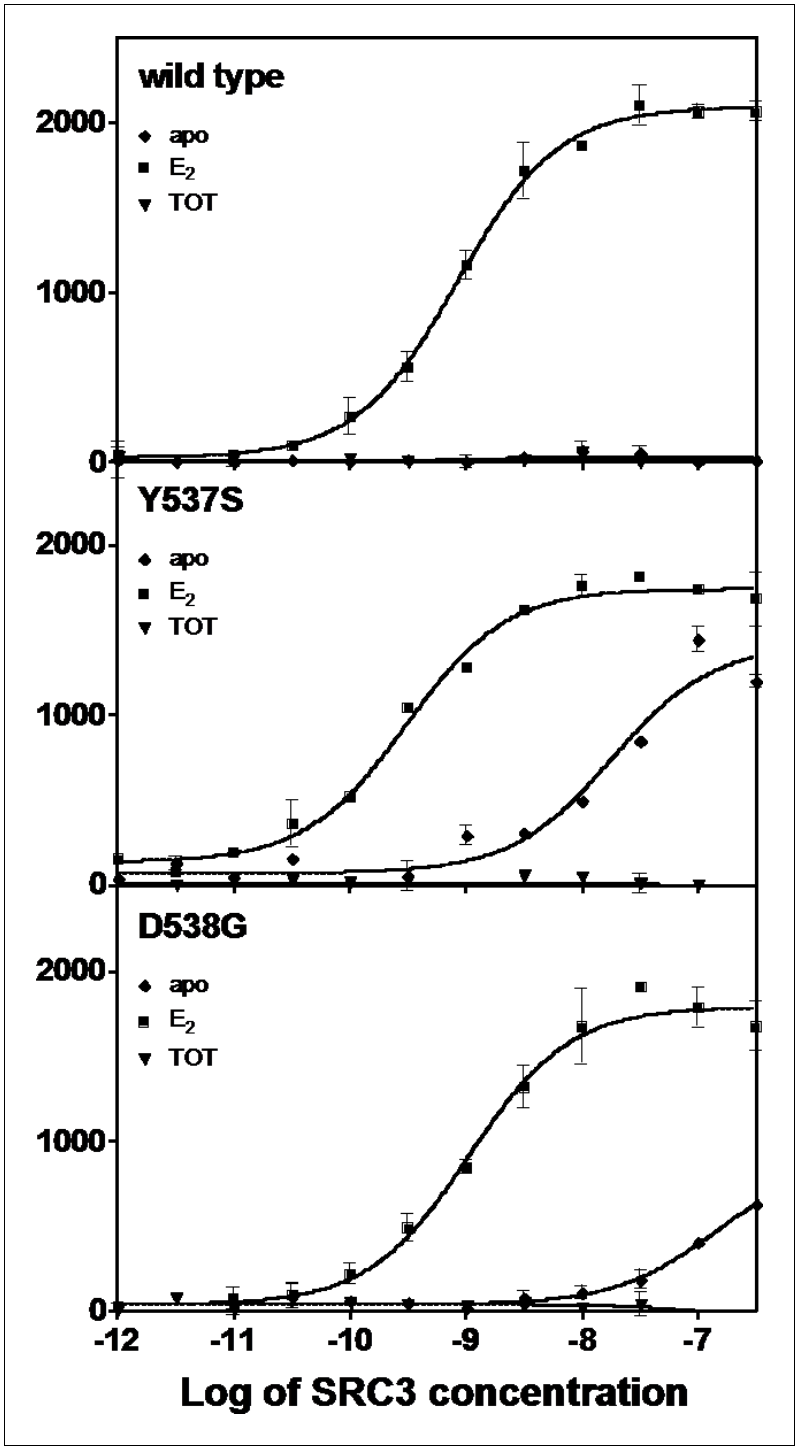

Figure 1. Binding of the SRC3 coactivator to WT, Y537S, or D538G ERα LBD in the absence or presence of E2 or TOT. LBD, ligand-binding domain.

DOI: https://doi.org/10.7554/eLife.12792.004

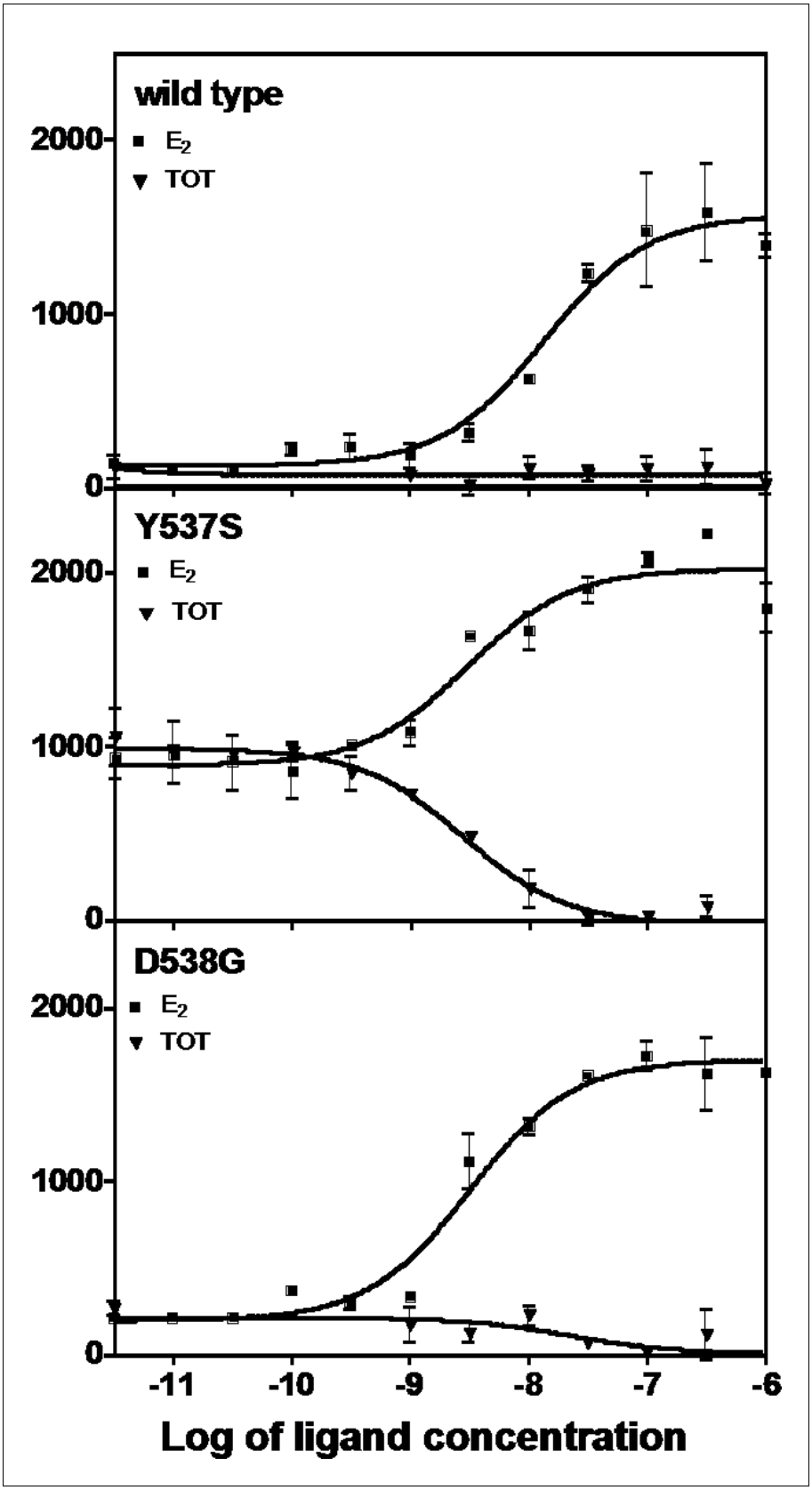

Figure 1—figure supplement 1. Binding of the SRC3 coactivator to WT, Y537S, or D538G mutant ERα LBD with increasing concentrations of E2 or TOT.
DOI: https://doi.org/10.7554/eLife.12792.005

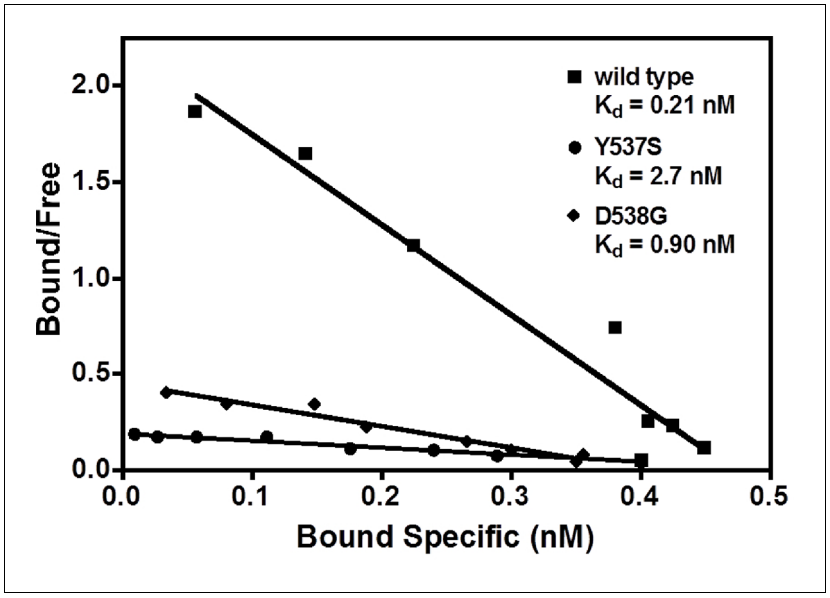

Figure 2. Determination of K_d values of estradiol (E2) binding to wild type, Y537S, and D538G LBDs, by a direct binding assay. All slopes had an r^2 of 0.95 or better; shown is a representative experiment. For details, see Methods. LBD, ligand-binding domain.

DOI: https://doi.org/10.7554/eLife.12792.006

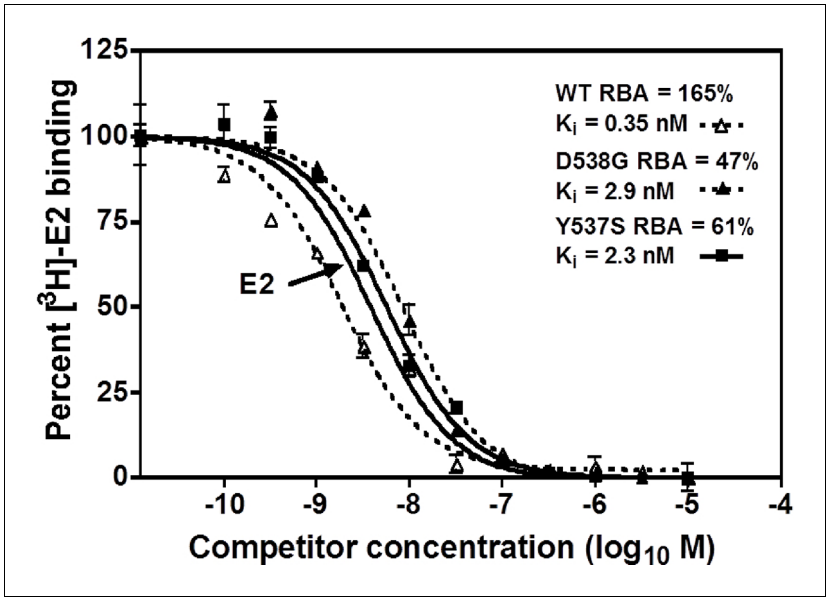

Figure 3. Relative binding affinity assay of wild type, Y537S, and D538G ligand-binding domains (LBDs), showing the TOT competition curves. With all proteins, the E2 curve is set to 100% and is shown only once. For details, see Methods.

DOI: https://doi.org/10.7554/eLife.12792.008

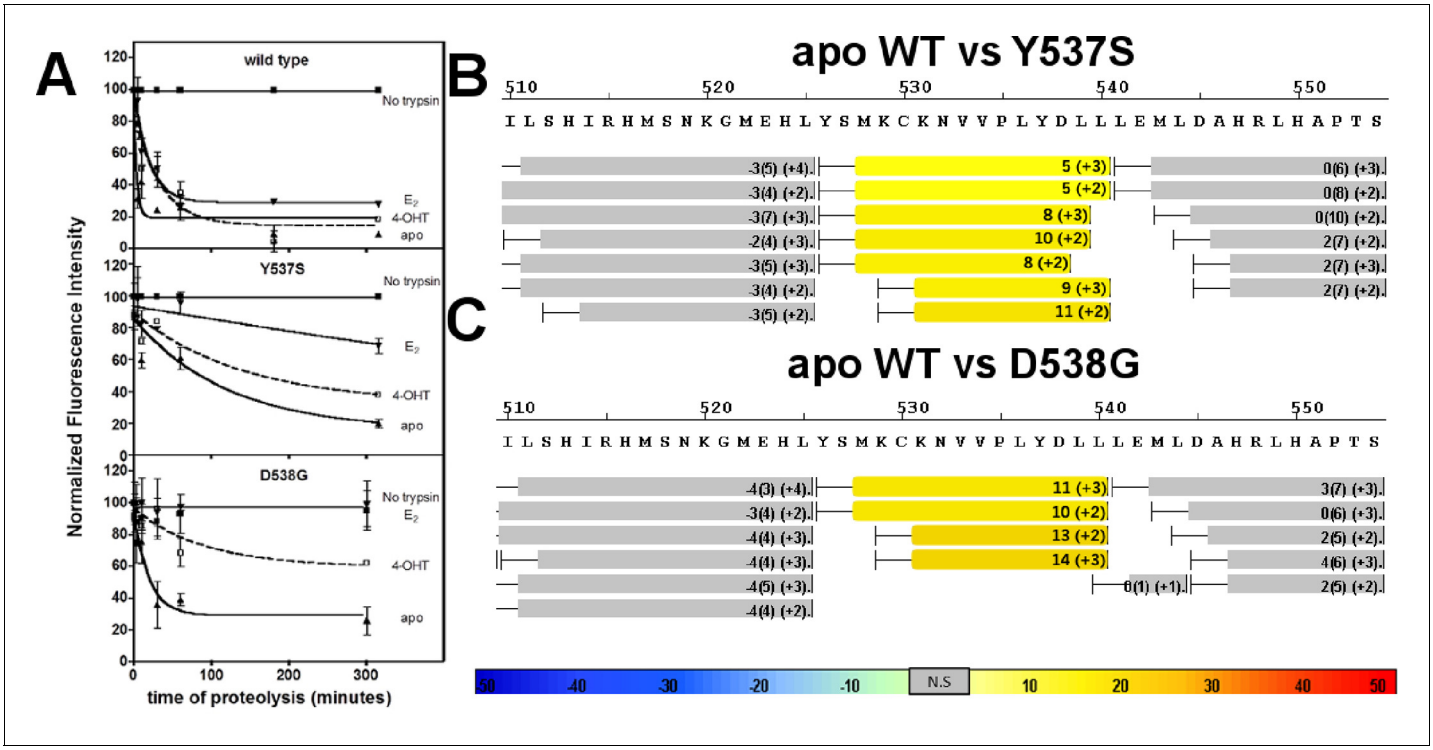

Figure 4. Conformational stability of WT and mutant ERα LBD H11-12 loop and H12. (**A**) Proteolytic susceptibility of the WT, Y537S, and D538G ERα LBD mutants in the *apo*, E2-bound, and TOT-bound states. (**B–C**) Deuterium uptake plot for the C-terminus of H11 along with the H11-12 loop and H12 for the *apo* WT vs Y537S ERα LBD (**B**), *apo* WT vs D538G ERα LBD (**C**). All HDX MS data represent an average of three replicates and are color coded from red to blue with warm colors representing increased conformational dynamics (red being the highest D2O uptake) and cool colors representing decreased conformational dynamics (blue being the lowest D2O uptake). All regions colored were determined to be statistically significant based on a paired two-tailed Students t-test. A legend is provided at the bottom. Grey indicates no statistically significant change between the two *apo* states. HDX, hydrogen/deuterium exchange; LBD, ligand-binding domain.

DOI: https://doi.org/10.7554/eLife.12792.009

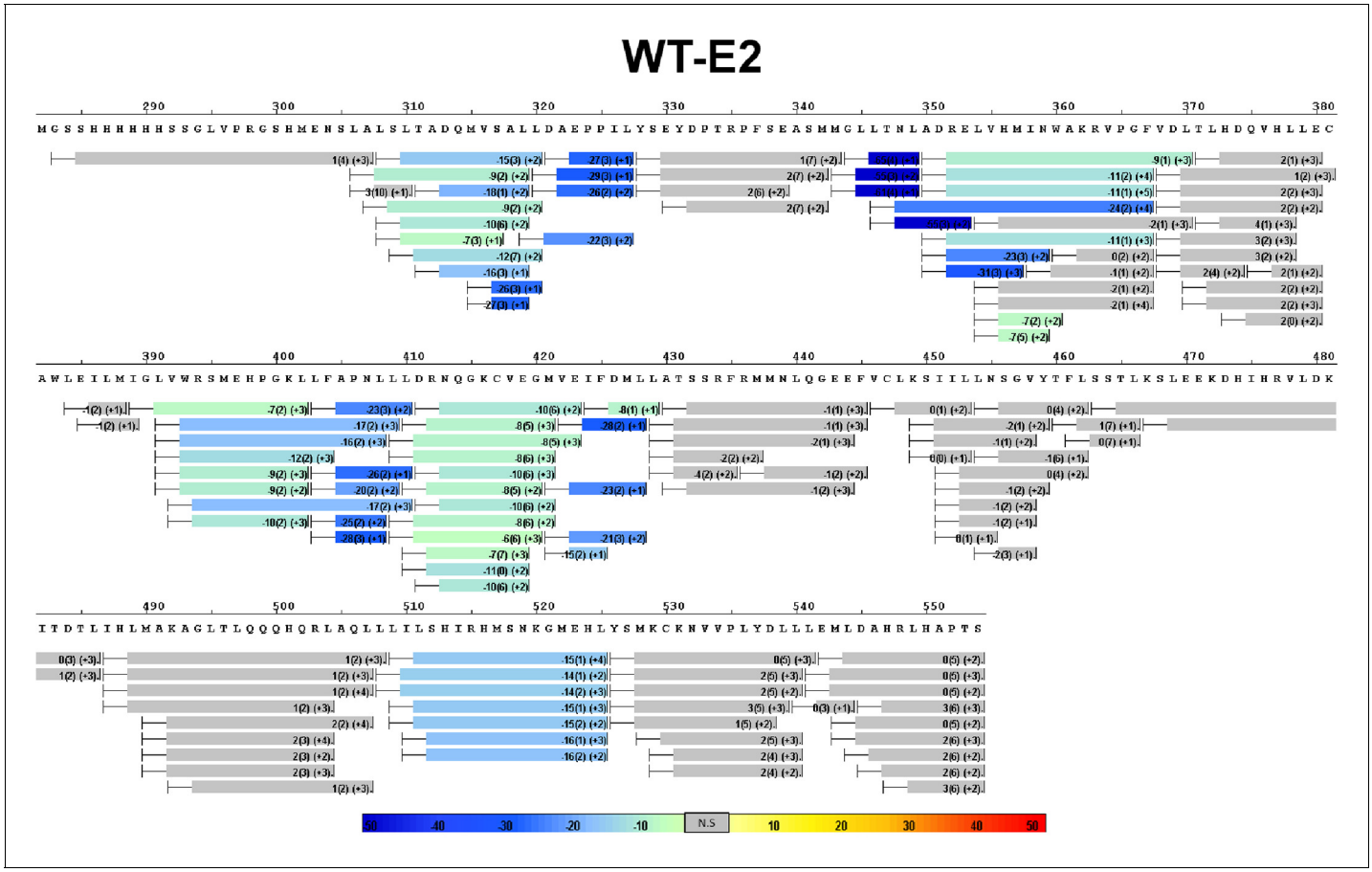

Figure 4—figure supplement 1. Complete differential amide HDX MS map of WT ERα LBD binding to E2.
DOI: https://doi.org/10.7554/eLife.12792.010

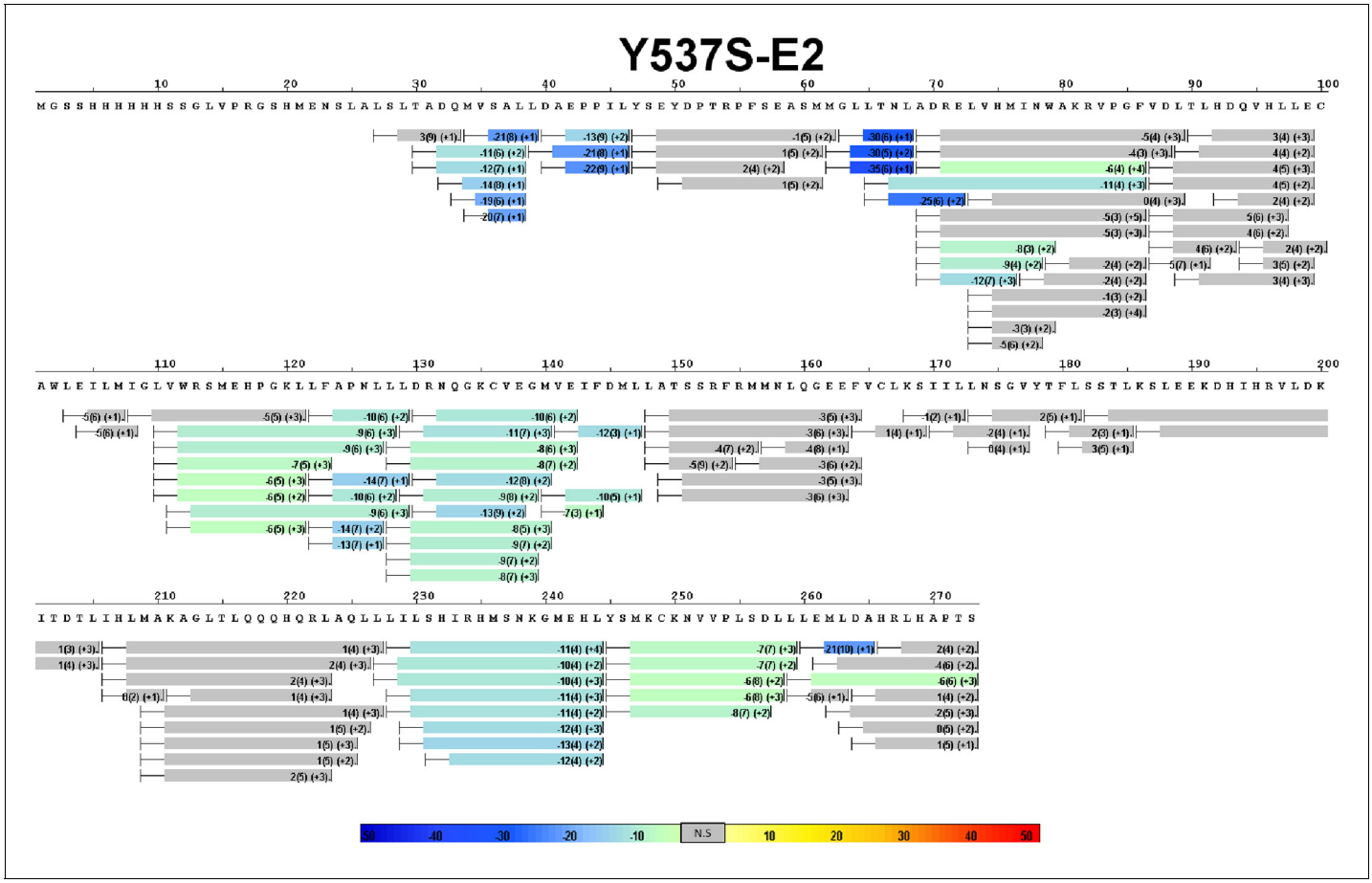

Figure 4—figure supplement 2. Complete differential amide HDX MS map of Y537S ERα LBD mutant binding to E2.
DOI: https://doi.org/10.7554/eLife.12792.011

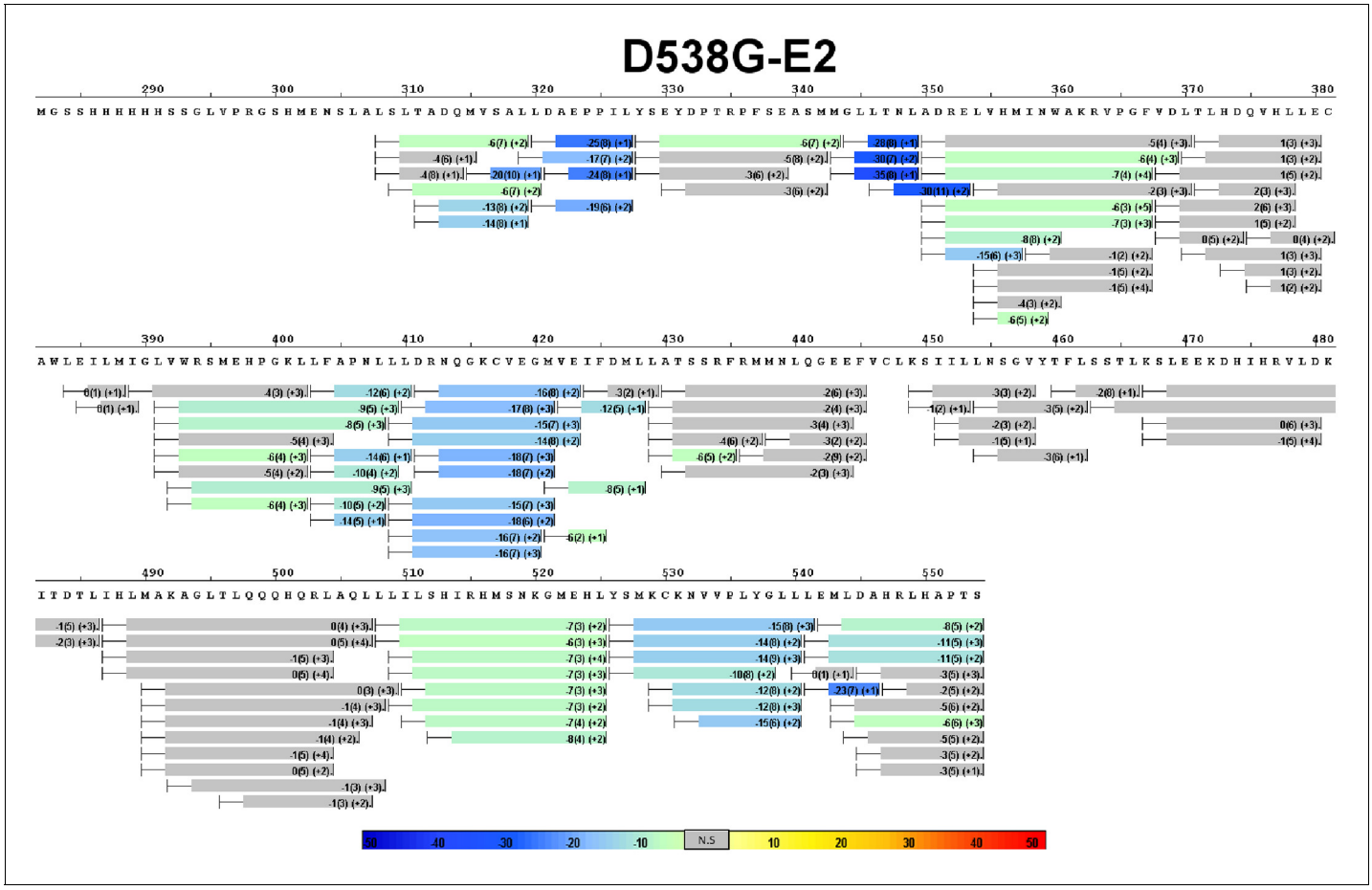

Figure 4—figure supplement 3. Complete differential amide HDX MS map of D538G ERα LBD mutant binding to E2.
DOI: https://doi.org/10.7554/eLife.12792.012

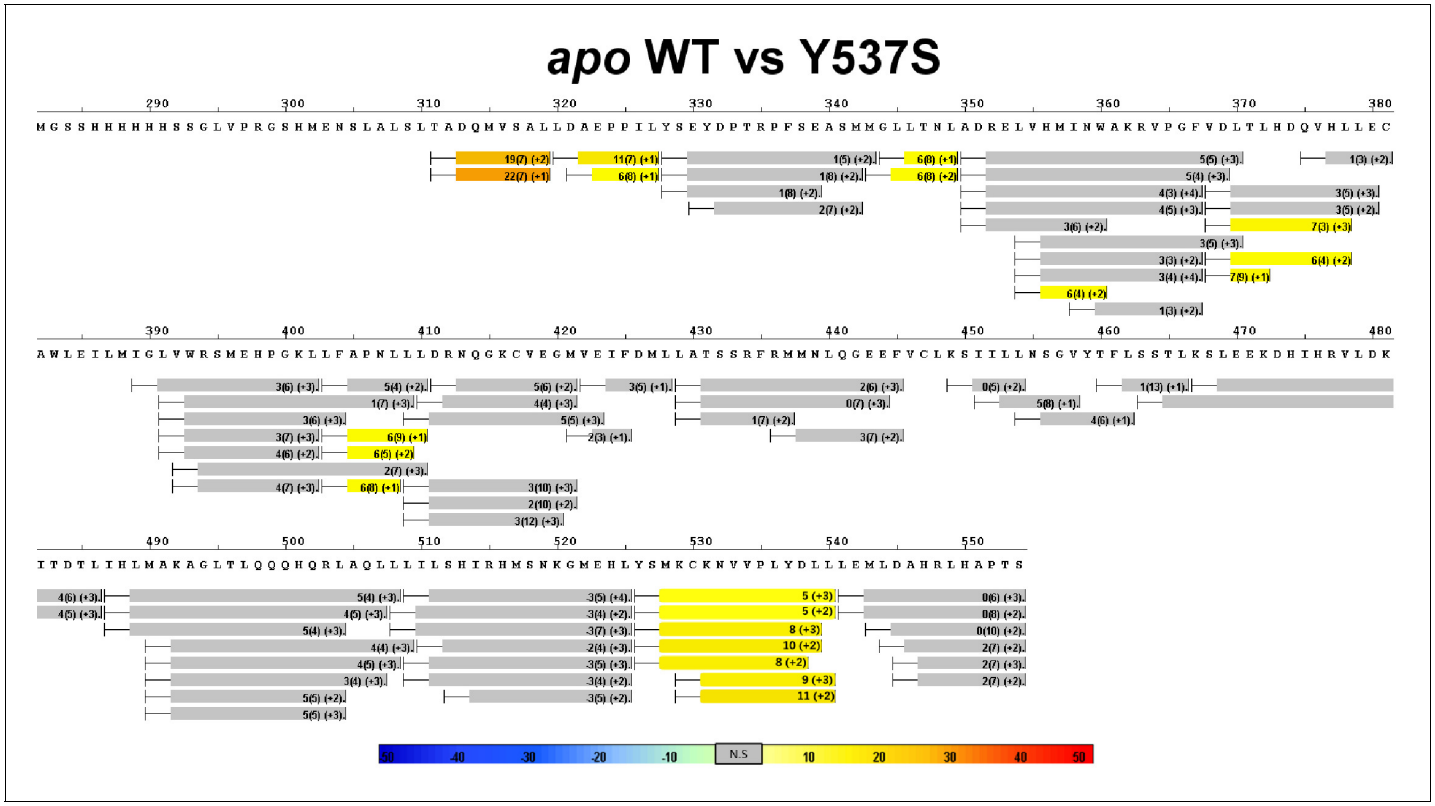

Figure 4—figure supplement 4. Complete differential HDX perturbation maps comparing the *apo* WT versus *apo* Y537S ERα LBD.
DOI: https://doi.org/10.7554/eLife.12792.013

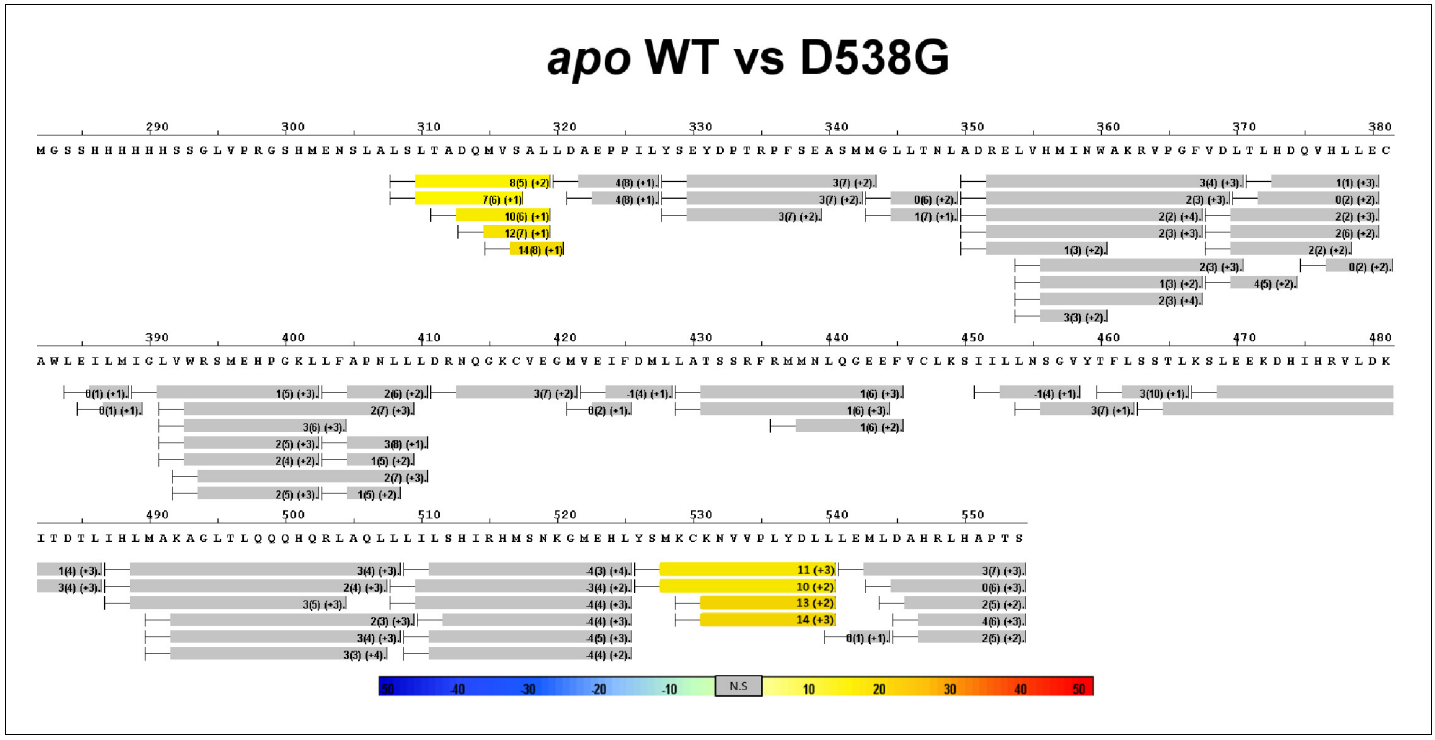

Figure 4—figure supplement 5. Complete differential HDX perturbation maps comparing the *apo* WT versus *apo* D538G ERα LBD.
DOI: https://doi.org/10.7554/eLife.12792.014

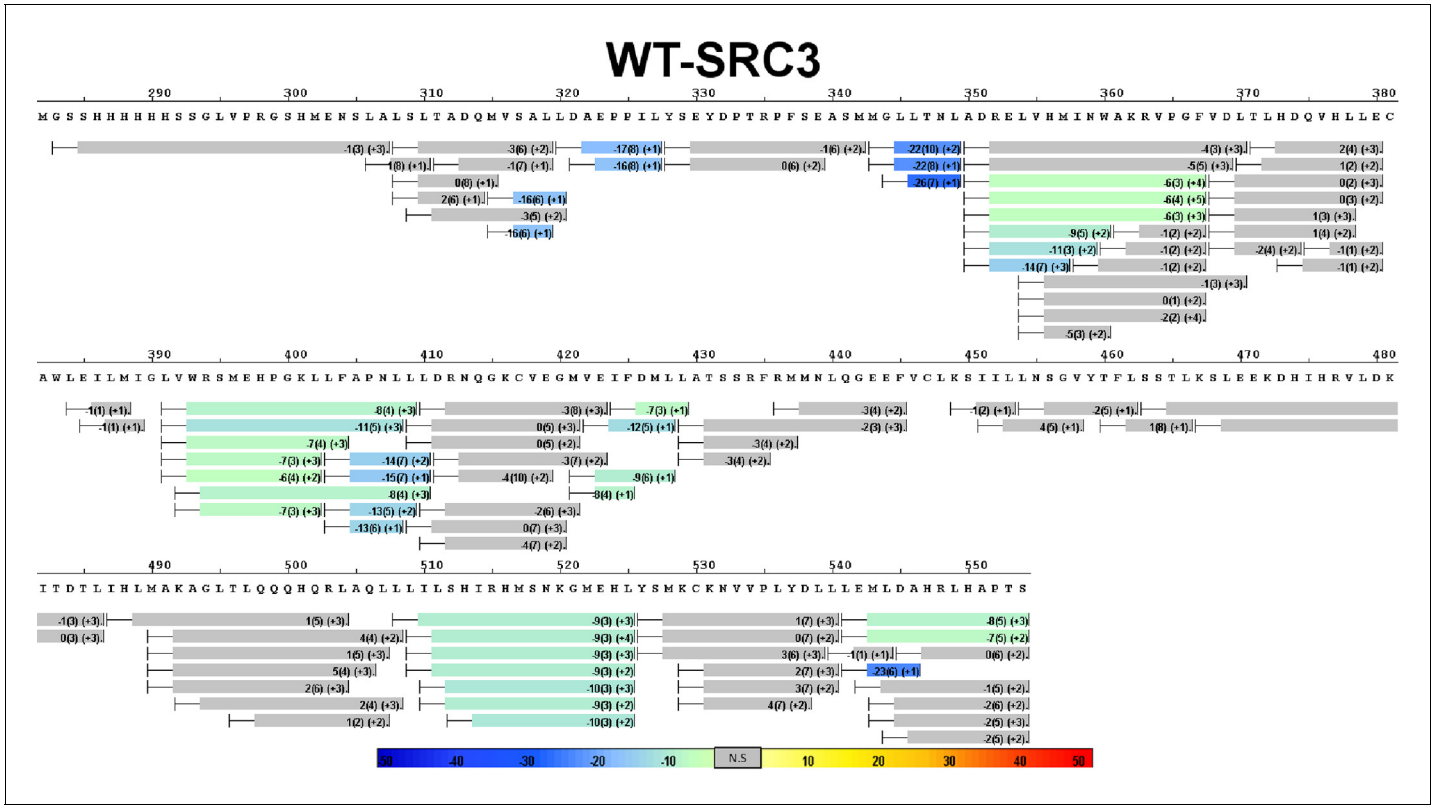

Figure 4—figure supplement 6. Complete differential HDX perturbation map of WT ERα LBD with SRC3-NRD.
DOI: https://doi.org/10.7554/eLife.12792.015

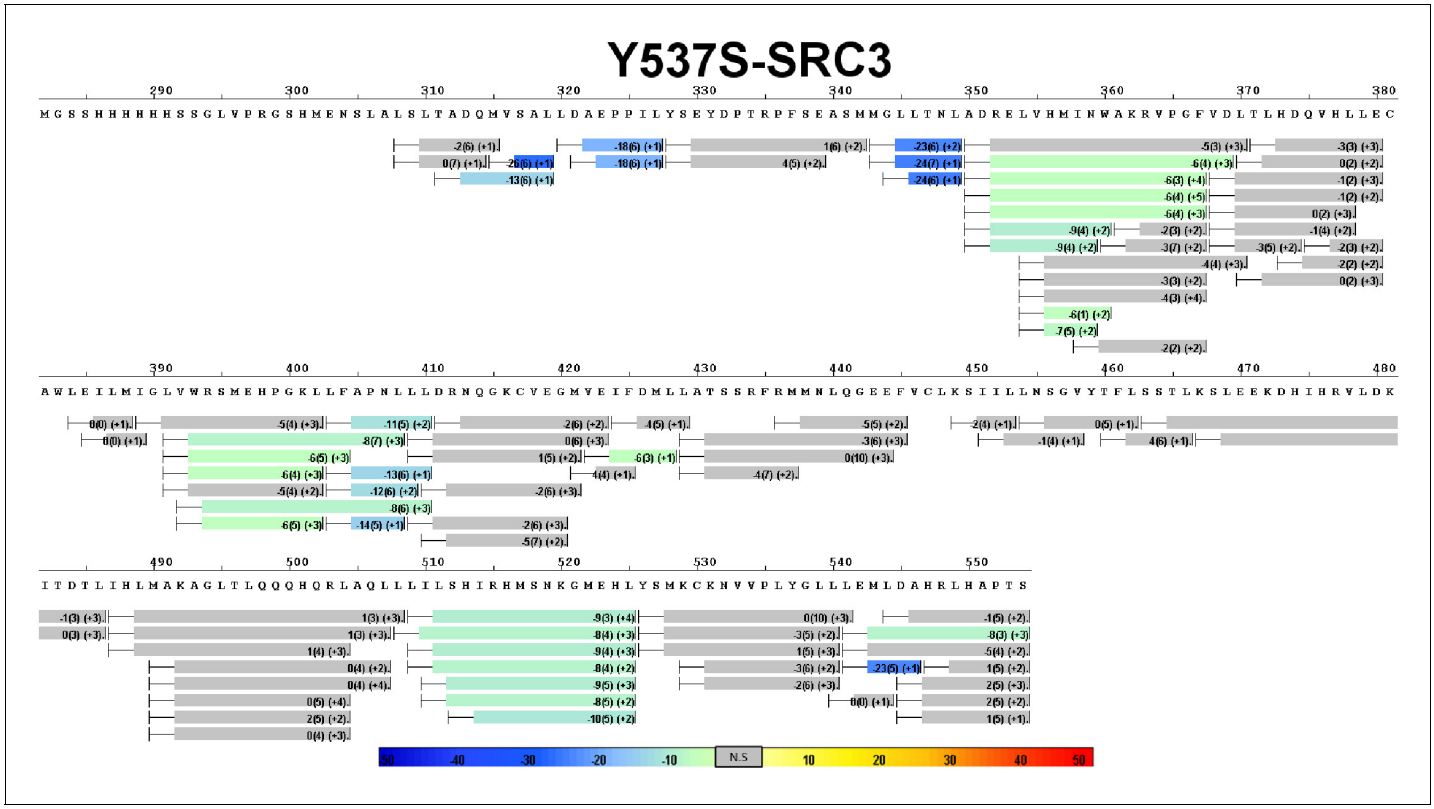

Figure 4—figure supplement 7. Complete differential HDX perturbation map of Y537S ERα LBD with SRC3-NRD.
DOI: https://doi.org/10.7554/eLife.12792.016

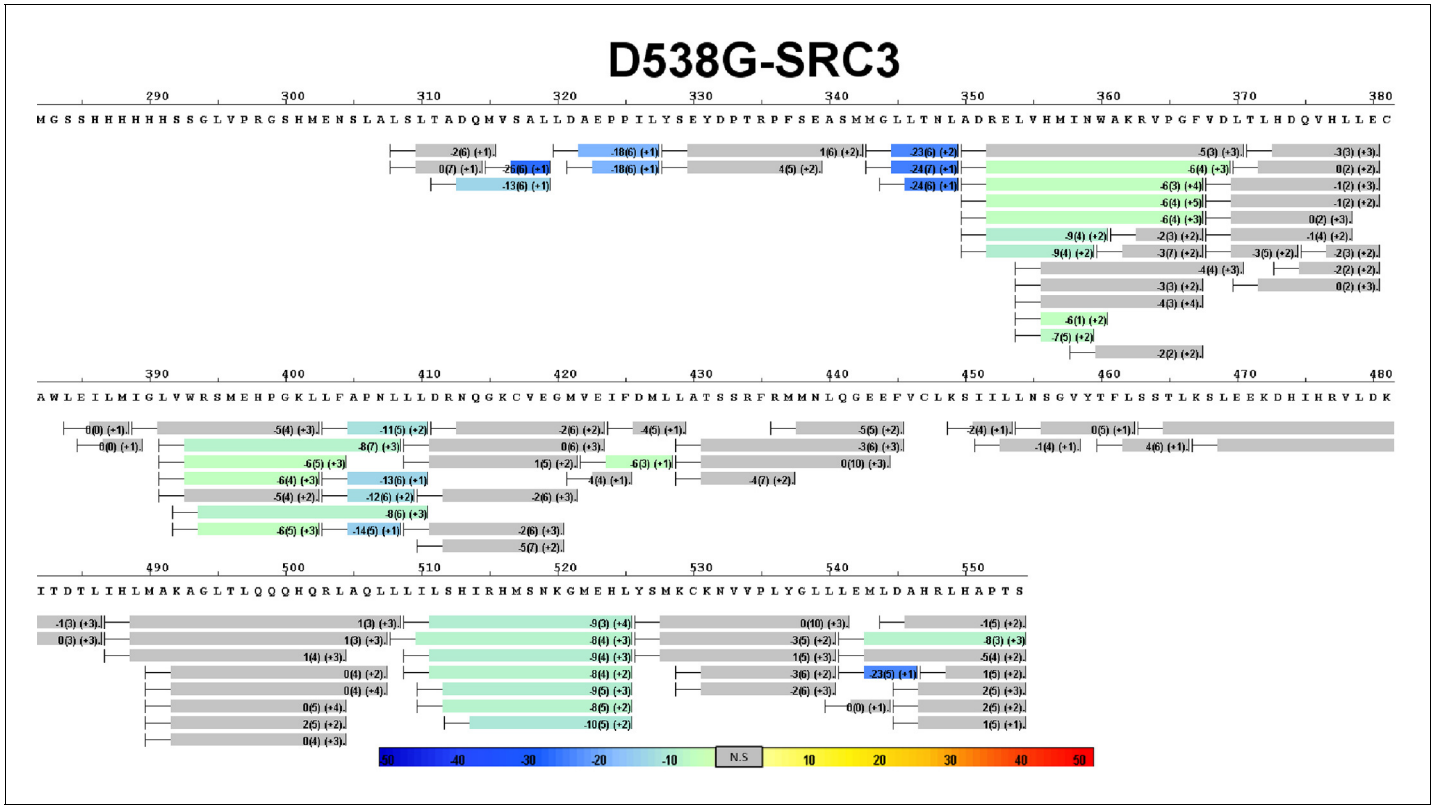

Figure 4—figure supplement 8. Complete differential HDX perturbation map of D538G ERα LBD with SRC3-NRD.
DOI: https://doi.org/10.7554/eLife.12792.017

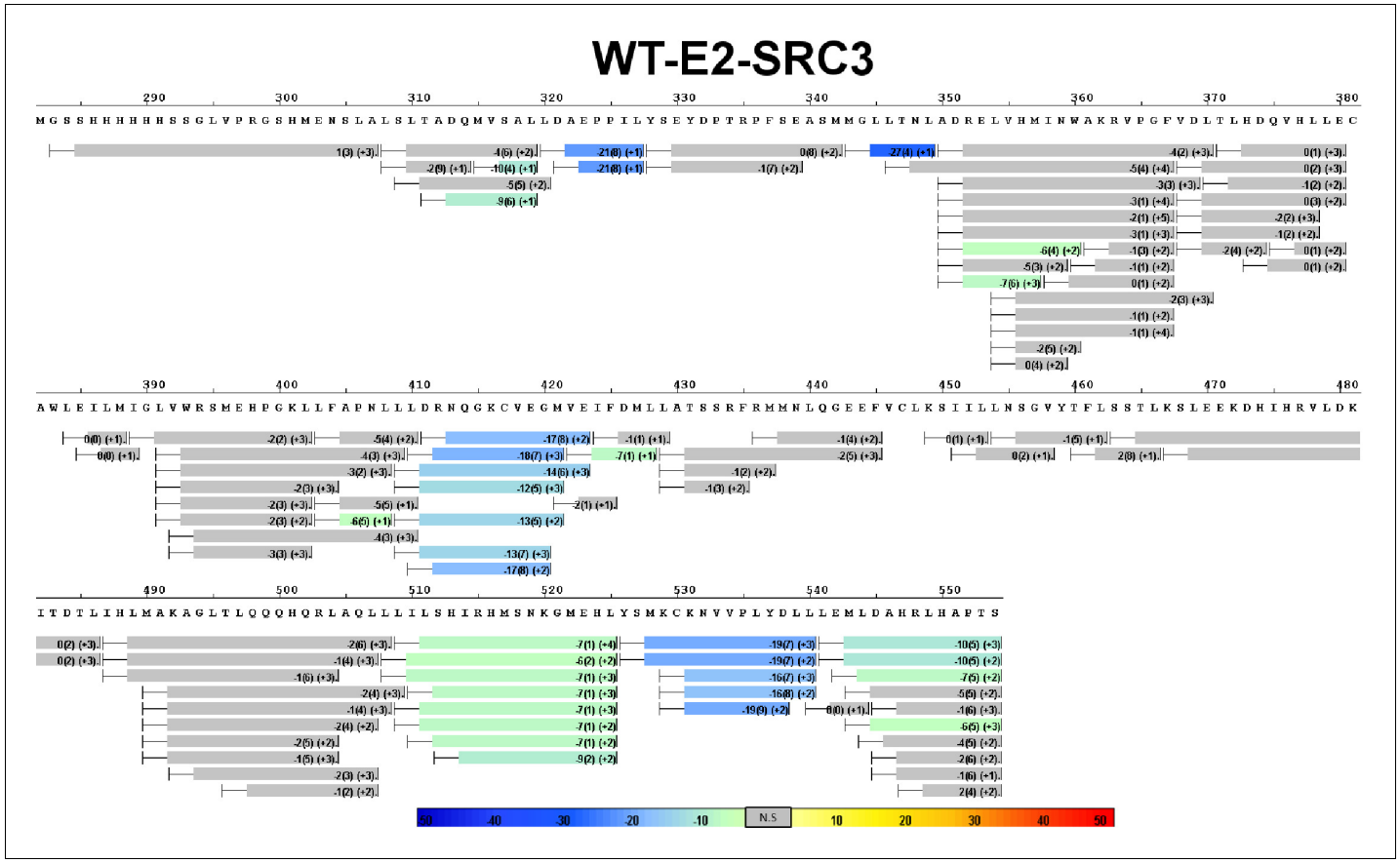

Figure 4—figure supplement 9. Complete differential HDX perturbation map of WT ERα LBD with E2 and SRC3-NRD.
DOI: https://doi.org/10.7554/eLife.12792.018

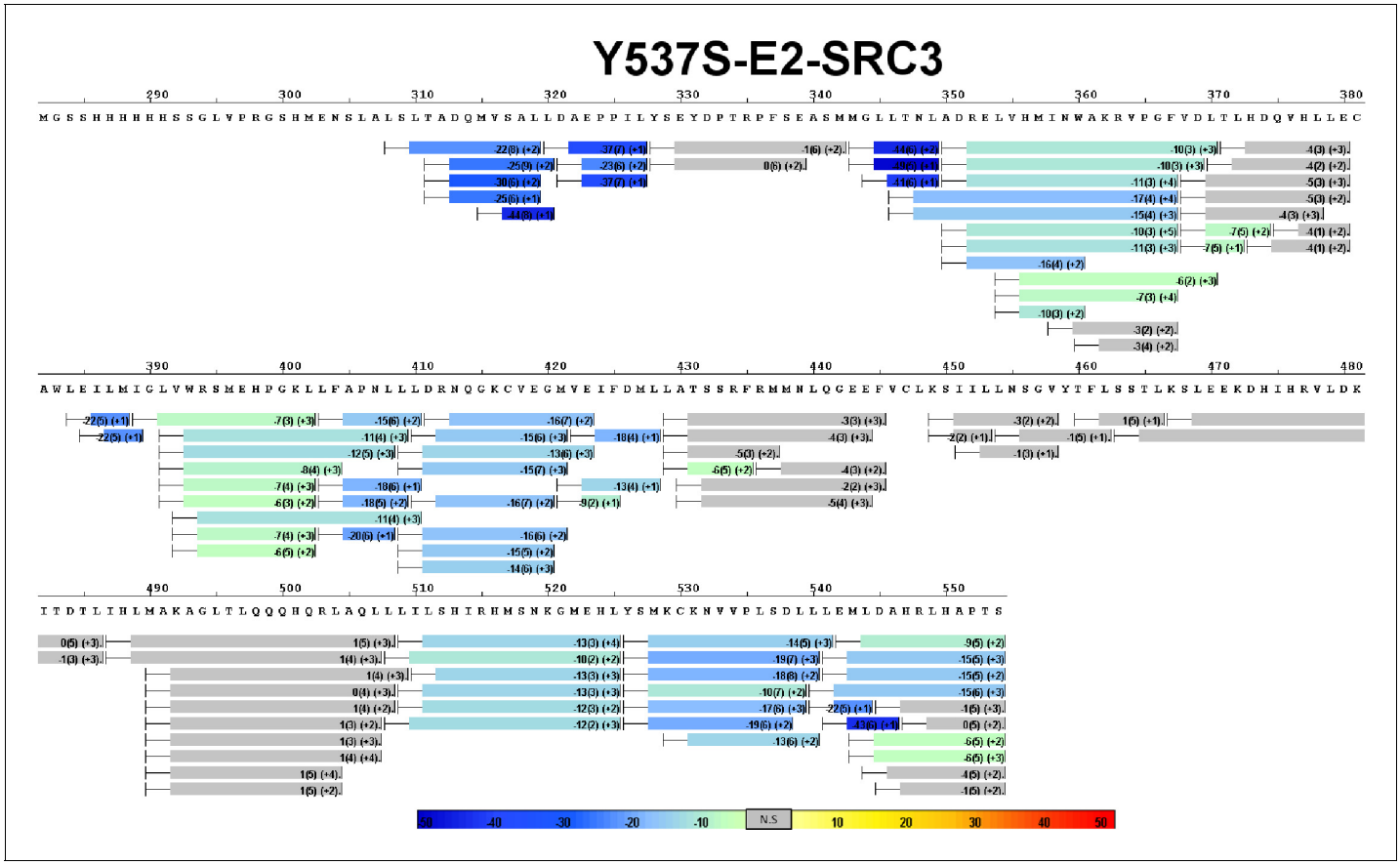

Figure 4—figure supplement 10. Complete differential HDX perturbation map of Y537S ERα LBD with E2 and SRC3-NRD.
DOI: https://doi.org/10.7554/eLife.12792.019

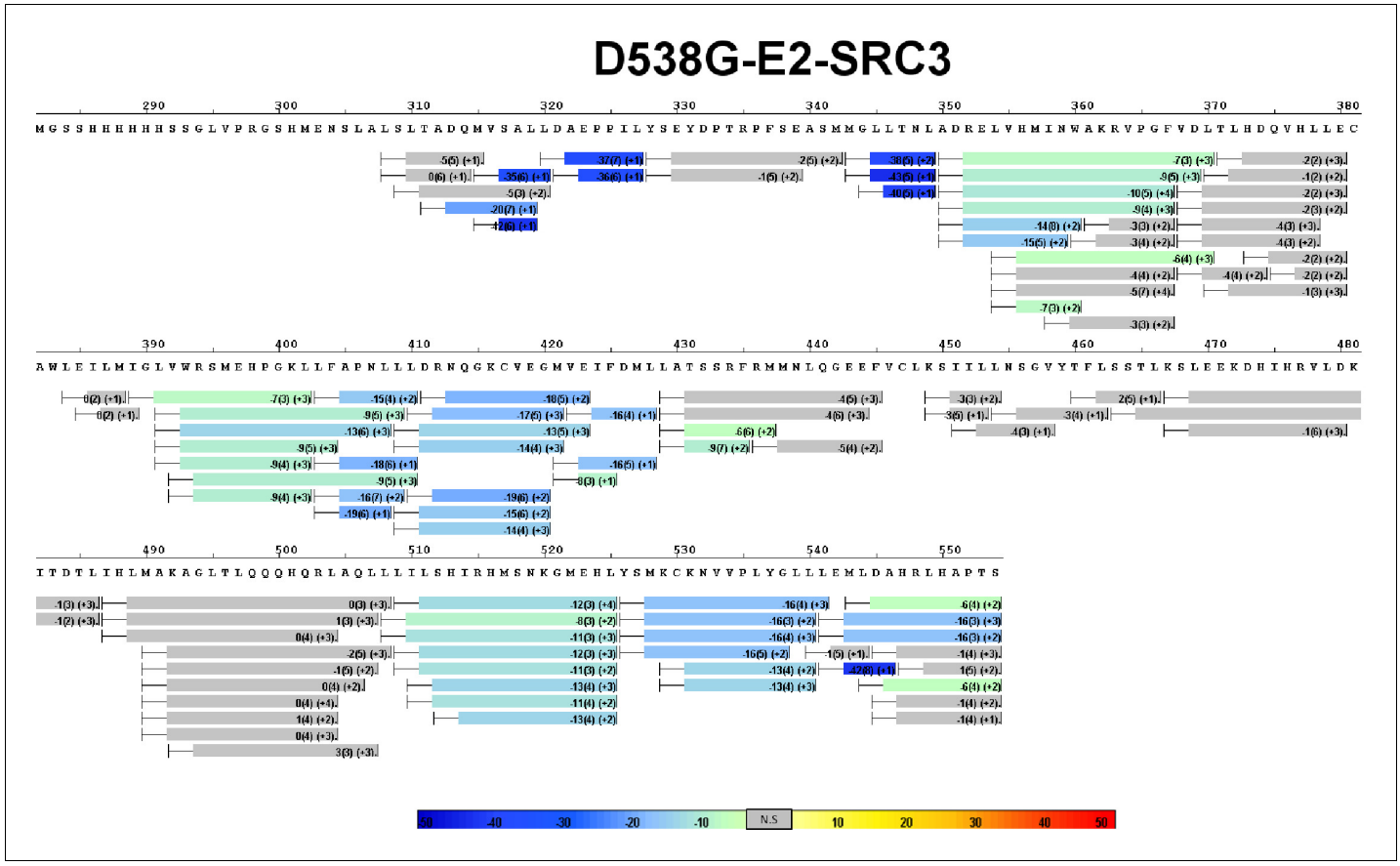

Figure 4—figure supplement 11. Complete differential HDX perturbation map of D538G ERα LBD with E2 and SRC3-NRD.
DOI: https://doi.org/10.7554/eLife.12792.020

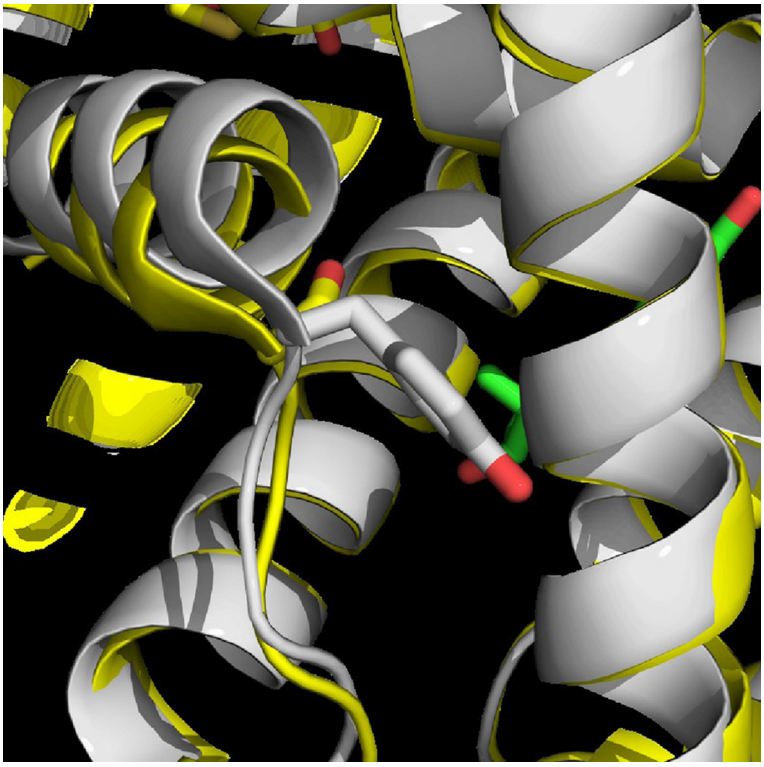

Figure 4—figure supplement 12. *apo* Y537S x-ray crystal structure (Yellow) (PDB: 2B23) superimposed with WT-E2 complex structure (White) (PDB: 1GWR).
DOI: https://doi.org/10.7554/eLife.12792.021

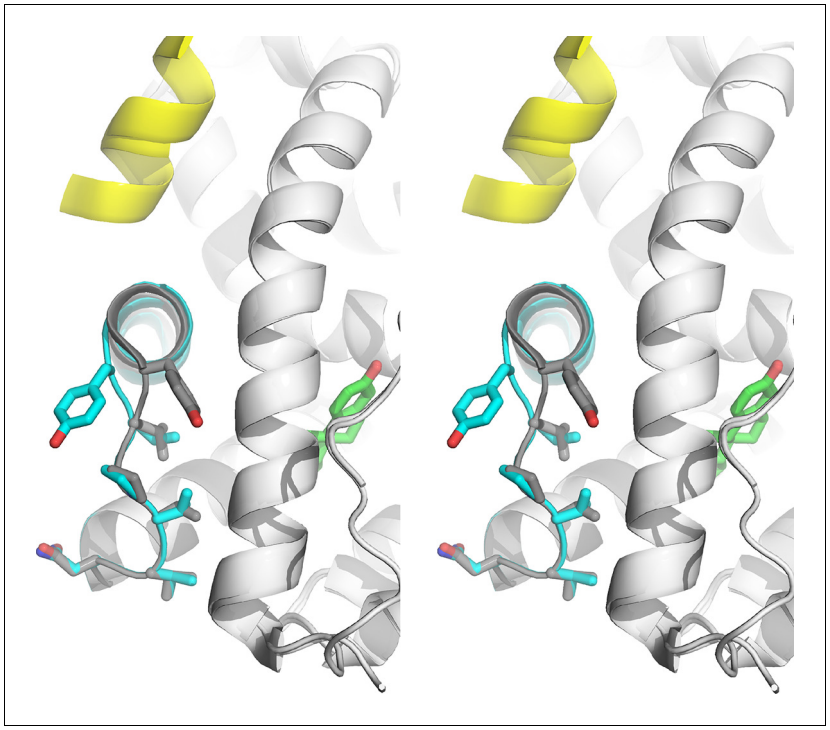

Figure 5. Stabilized D538G agonist state. Superposition stereo-view image of the residues comprising the H11-12 loop (531–537) of monomer A of the D538G-E2 (cyan) overlaid with monomer A of the WT-E2 structure (PDB: 1GWR). E2 is represented as green sticks. Coactivator peptide is shown as light-yellow ribbon.

DOI: https://doi.org/10.7554/eLife.12792.023

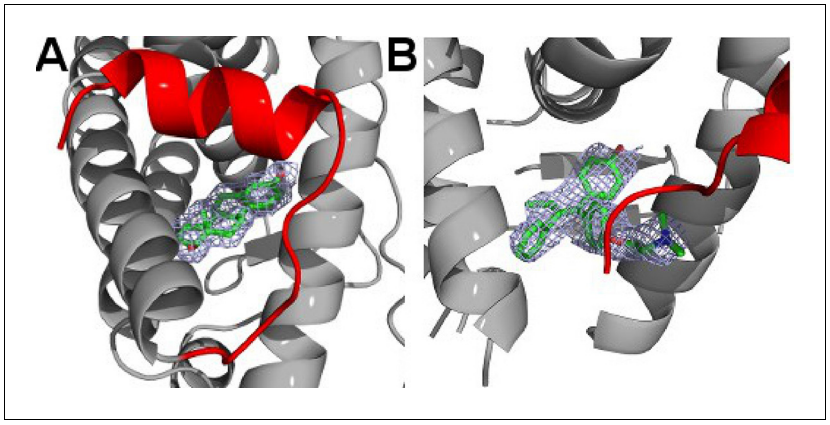

Figure 5—figure supplement 1. Simulated annealing composite omit maps for the E2 (**A**) and TOT (**B**)-bound D538G ERα LBD crystal structures contoured to 1.5σ. E2 and TOT are shown as sticks, helix 12 is highlighted in red, and electron density is shown as a blue cage. LBD, ligand-binding domain.

DOI: https://doi.org/10.7554/eLife.12792.024

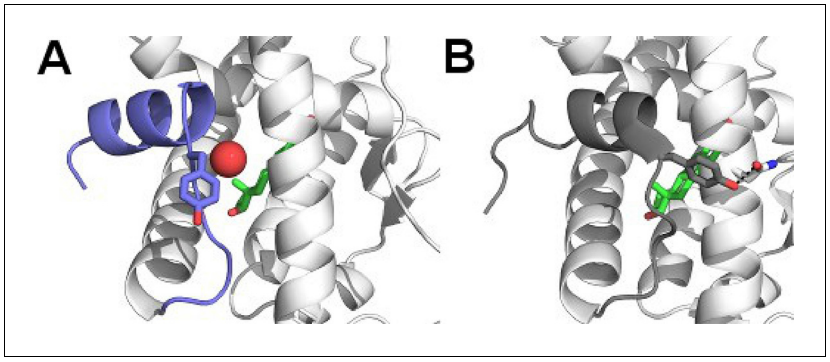

Figure 5—figure supplement 2. Y537 orientations for D538G and WT LBD. (**A**) Y537 of the D538G-E2 structure rotates toward solvent and is replaced by a well ordered water molecule (sphere), location of the ligand-binding site is shown with estradiol as green sticks, H11-12 loop and H12 shown as dark-blue. (**B**) Y537 is buried toward Helix 3 in every WT structure, forming a hydrogen bond with N348 (PDB: 1GWR).
DOI: https://doi.org/10.7554/eLife.12792.025

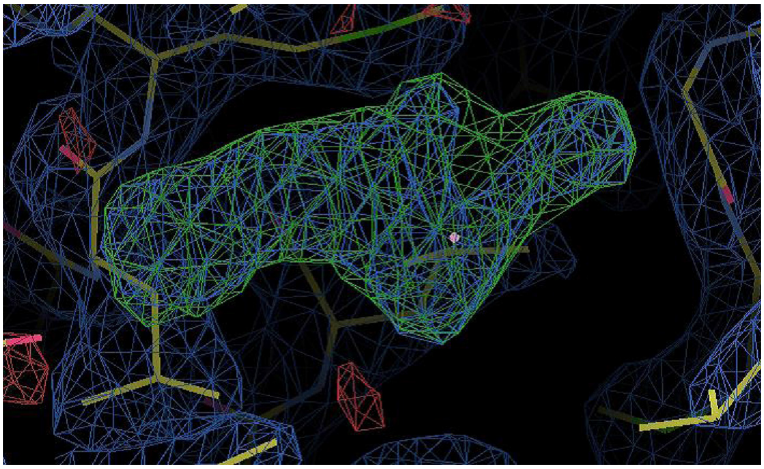

Figure 5—figure supplement 3. Density of an unidentified small molecule in the ligand-binding site of the *apo* D538G x-ray crystal structure.
DOI: https://doi.org/10.7554/eLife.12792.026

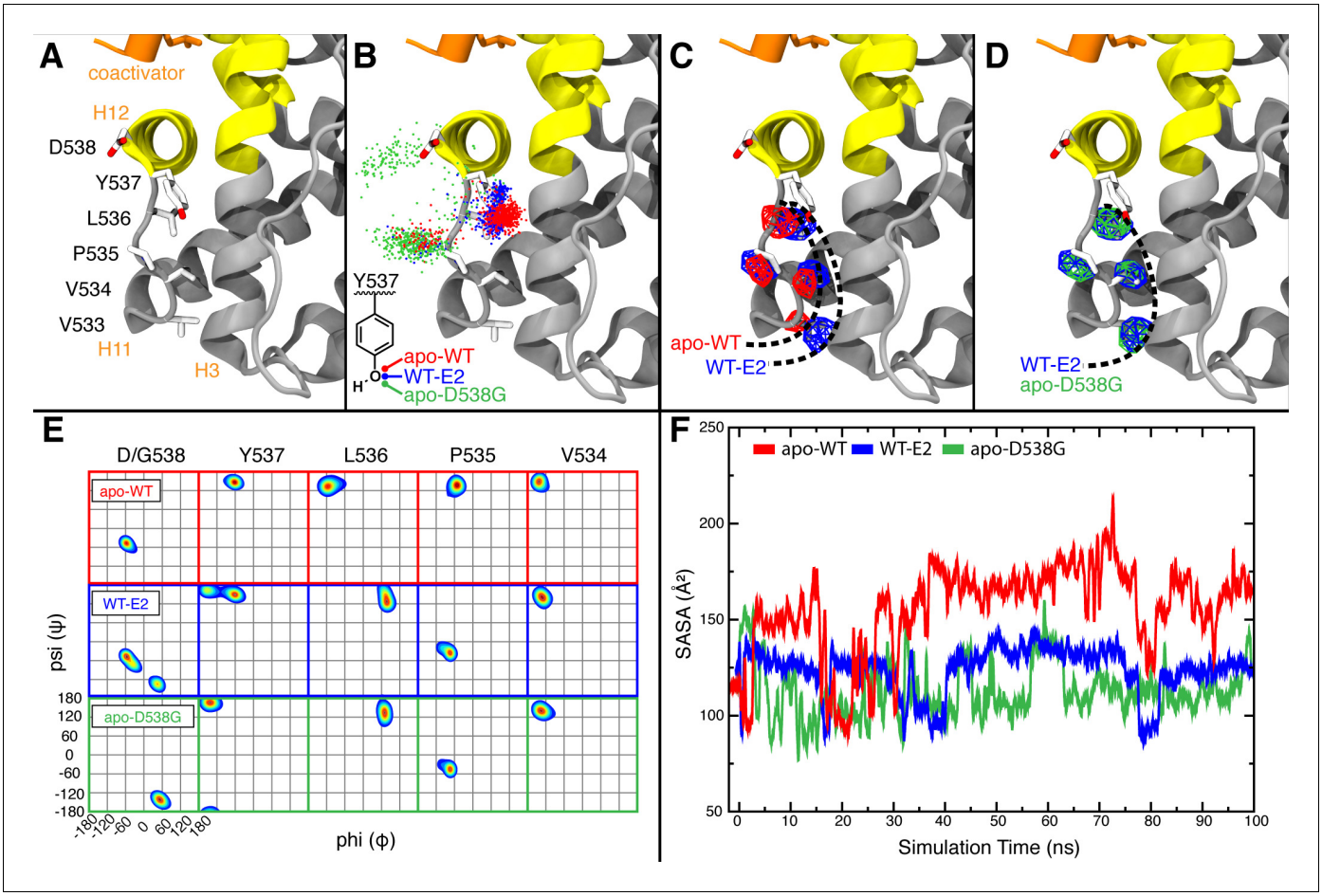

Figure 6. Visualization of H11-12 loop dynamics. (**A**) H11-12 loop of WT ERα LBD-E2 complex. (**B**) Superimposing the position of the phenolic oxygen of Y537 at 0.1-ns intervals for *apo* WT (red), WT-E2 (blue), and *apo* D538G mutant (green). (**C**) Mapping the mass density isosurface (0.75, i.e., 25th percentile) of the hydrophobic side chains in the linker region (V533, V534, P535, and L536). (**D**) Side-chain packing of the *apo* D538G structure compared to WT-E2. (**E**) Ramachandran analysis of residues 534–538 for the *apo* WT, WT-E2, and *apo* D538G MD simulations. (**F**) Time series of the solvent accessible surface area (SASA) for hydrophobic loop residues (533–536). LBD, ligand binding domain.

DOI: https://doi.org/10.7554/eLife.12792.027

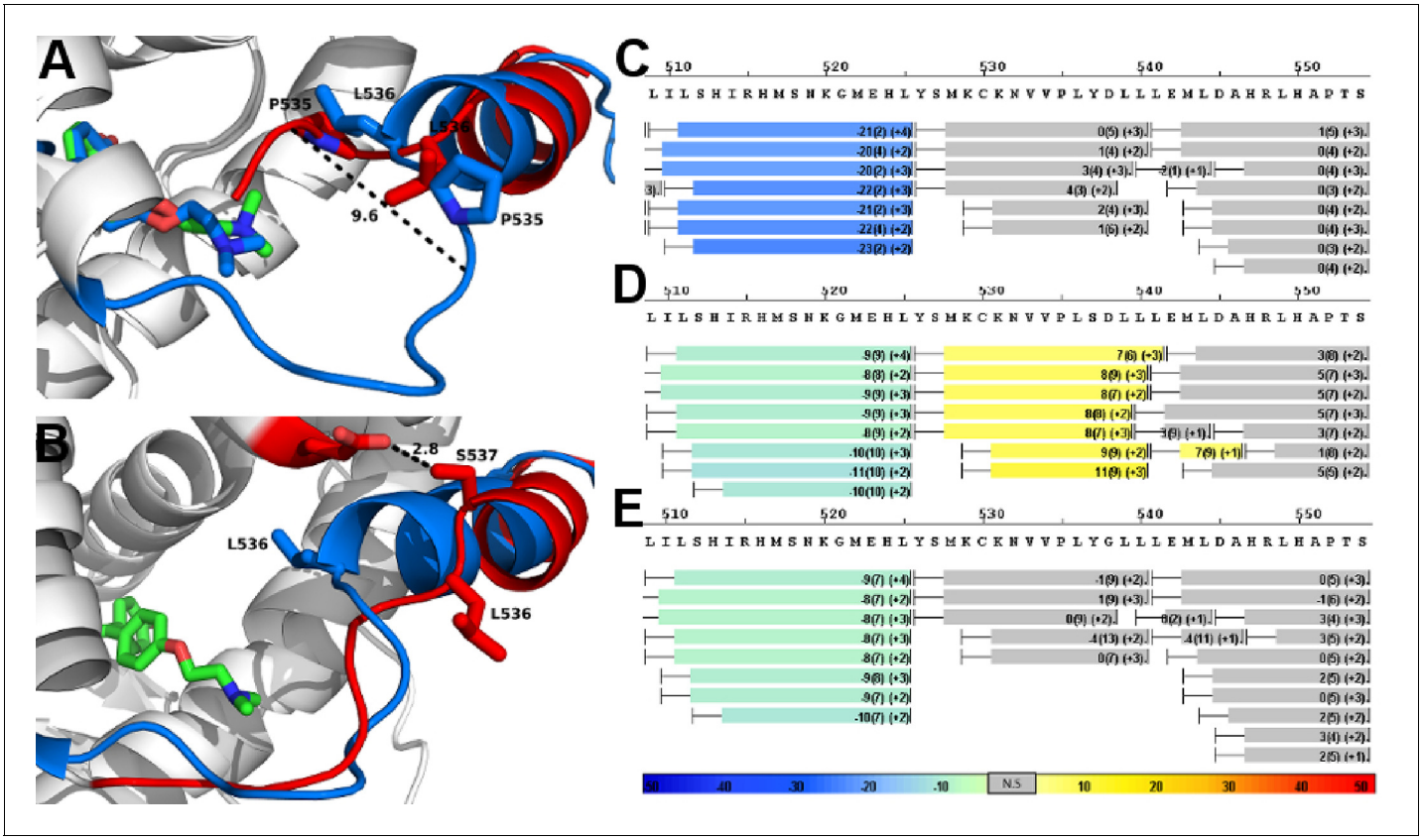

Figure 7. Alterations to the D538G and Y537S antagonist conformational states. (**A**) Superposition of monomer A for the 538G-TOT structure with the WT (3ERT). TOT and residues 530–550 of the WT (blue) (PDB: 3ERT), TOT of D538G (green), residues 531–550 (red). (**B**) Predicted conformational alterations in H12 in the Y537S-TOT structure (red) compared to the WT-TOT (blue). (**C**) HDX-MS of the WT-TOT complex for H11 through H12 regions. (**D**) HDX-MS of Y537S-TOT complex for H11 through H12 regions. (**E**) HDX-MS of the D538G-TOT complex for H11 through H12 regions. HDX data is color coded as in 2C. See methods for more details on coloring scheme. HDX-MS, hydrogen/deuterium exchange mass spectrometry; LBD, ligand binding domain.

DOI: https://doi.org/10.7554/eLife.12792.028

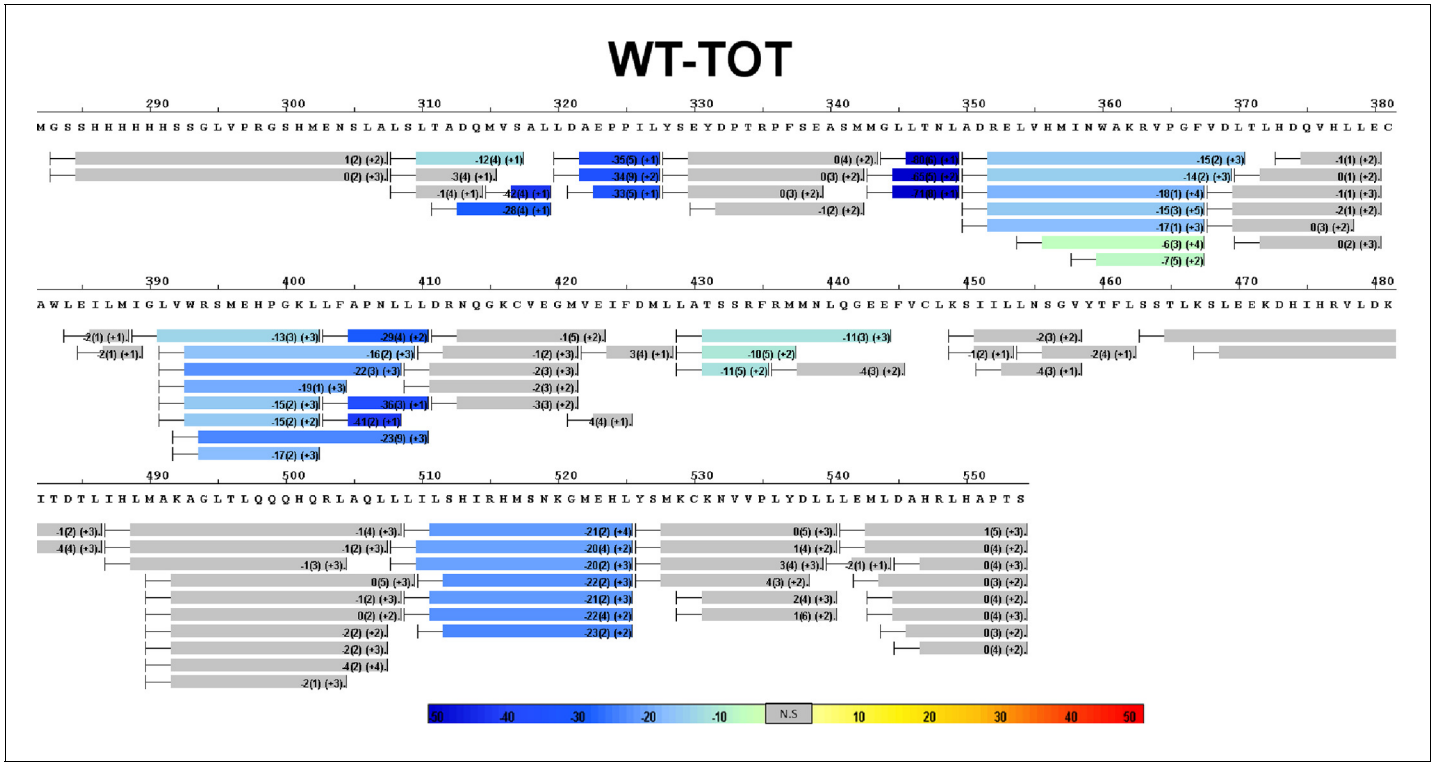

Figure 7—figure supplement 1. Complete differential amide HDX-MS map of WT ERα LBD binding to TOT.
DOI: https://doi.org/10.7554/eLife.12792.029

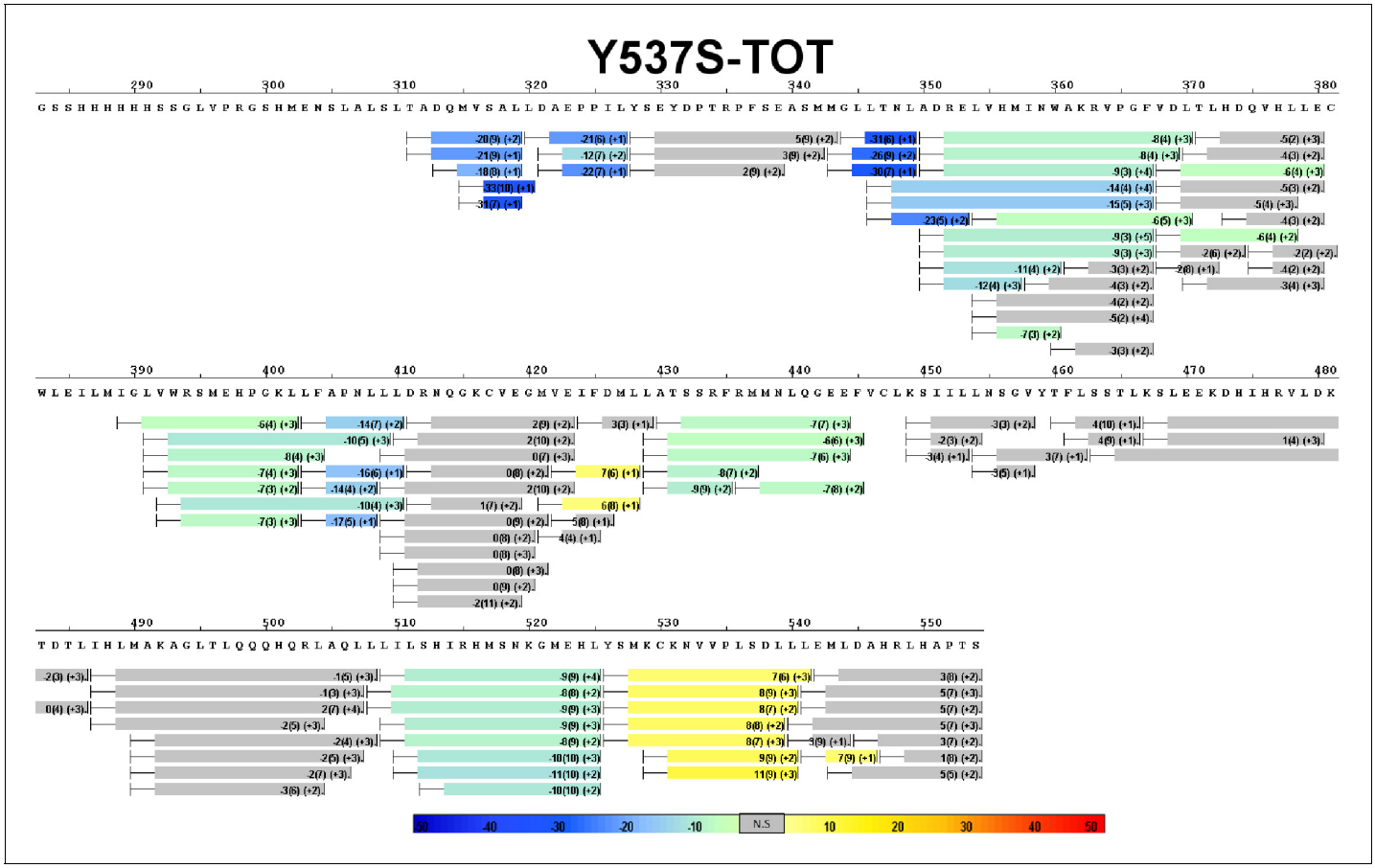

Figure 7—figure supplement 2. Complete differential amide HDX-MS map of Y537S ERα LBD mutant binding to TOT.
DOI: https://doi.org/10.7554/eLife.12792.030

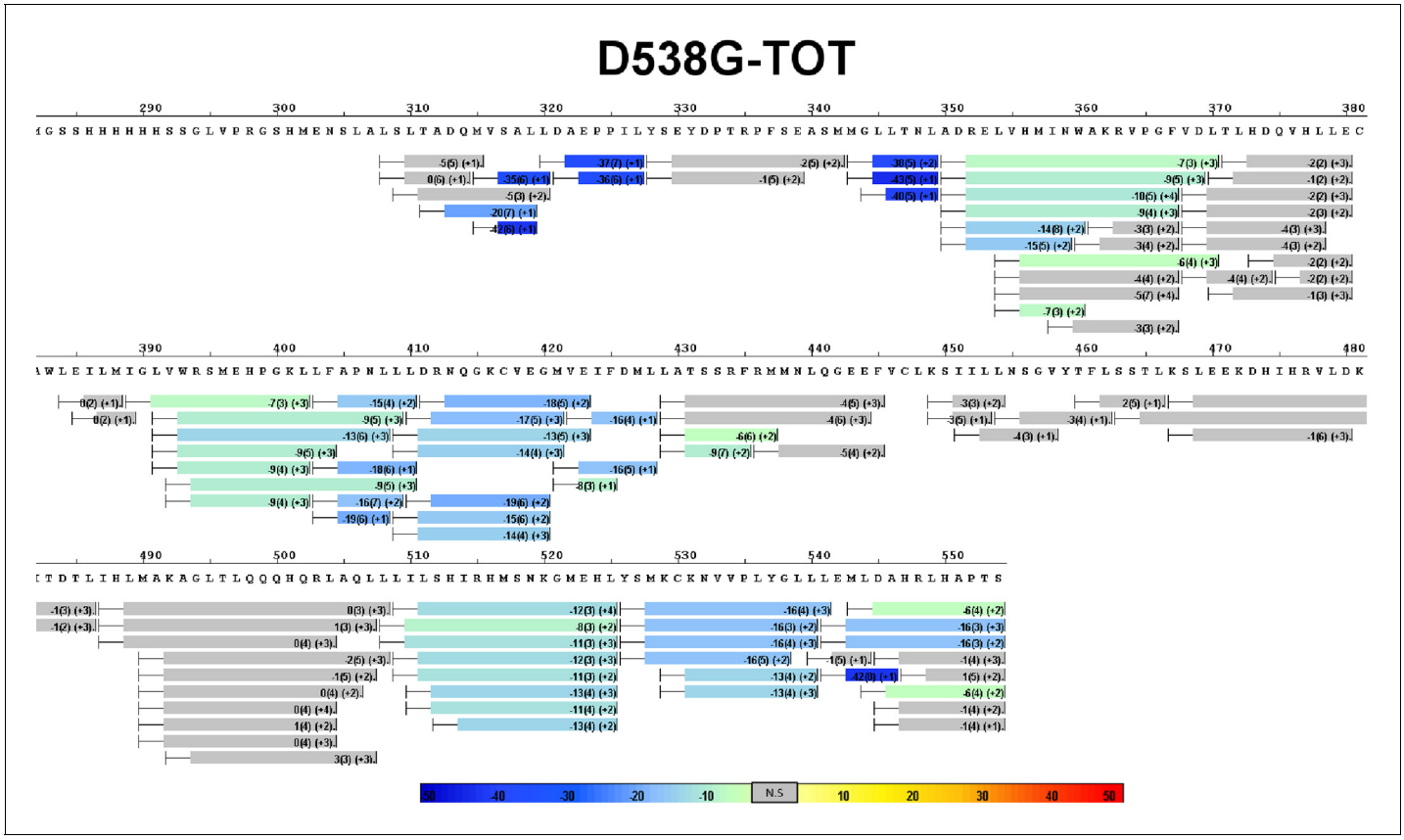

Figure 7—figure supplement 3. Complete differential amide HDX-MS map of D538G ERα LBD mutant binding to TOT.
DOI: https://doi.org/10.7554/eLife.12792.031

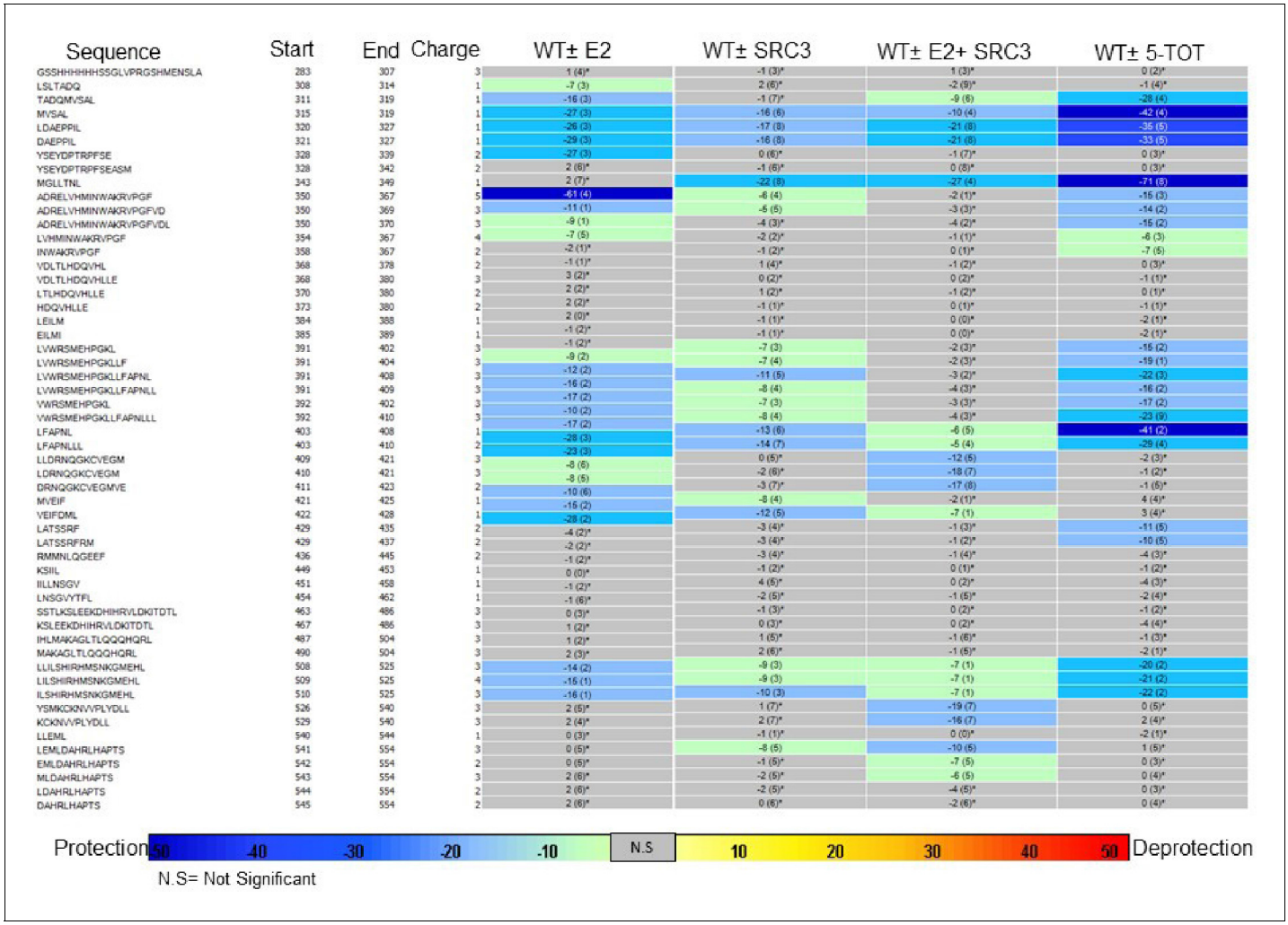

Figure 7—figure supplement 4. Experiment comparison view comparing the differential HDX behavior of *apo* WT ERα LBD in the presence of various ligands or coactivator.

DOI: https://doi.org/10.7554/eLife.12792.032

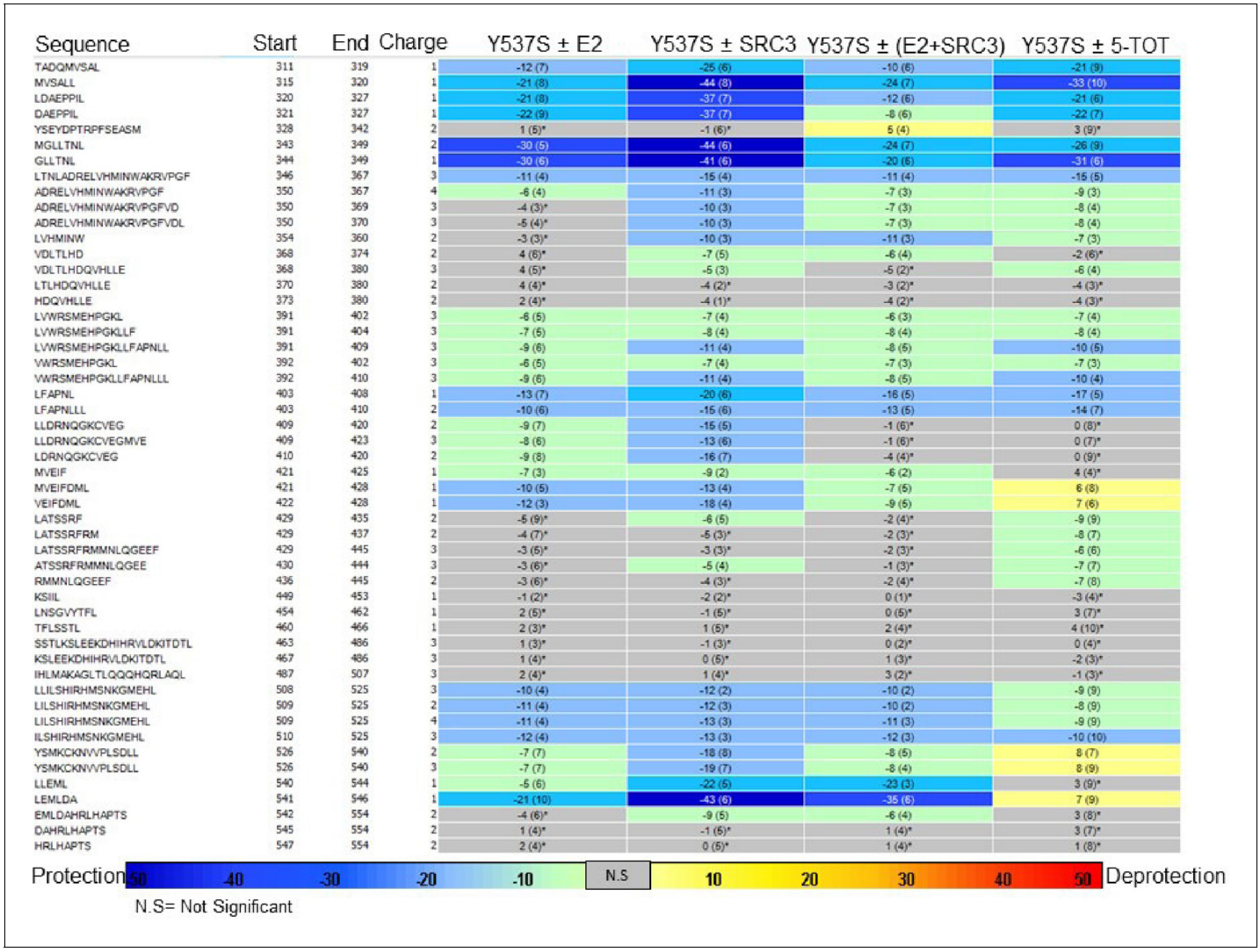

Sequence	Start	End	Charge	Y537S ± E2	Y537S ± SRC3	Y537S ± (E2+SRC3)	Y537S ± 5-TOT
TADQMVSAL	311	319	1	-12 (7)	-25 (6)	-10 (6)	-21 (9)
MVSALL	315	320	1	-21 (8)	-44 (8)	-24 (7)	-33 (10)
LDAEPPIL	320	327	1	-21 (8)	-37 (7)	-12 (6)	-21 (6)
DAEPPIL	321	327	1	-22 (9)	-37 (7)	-8 (6)	-22 (7)
YSEYDPTRPFSEASM	328	342	2	1 (5)*	-1 (6)*	5 (4)	3 (9)*
MGLLTNL	343	349	2	-30 (5)	-44 (6)	-24 (7)	-26 (9)
GLLTNL	344	349	1	-30 (6)	-41 (6)	-20 (6)	-31 (6)
LTNLADRELVHMINWAKRVPGF	346	367	3	-11 (4)	-15 (4)	-11 (4)	-15 (5)
ADRELVHMINWAKRVPGF	350	367	4	-6 (4)	-11 (3)	-7 (3)	-9 (3)
ADRELVHMINWAKRVPGFVD	350	369	3	-4 (3)*	-10 (3)	-7 (3)	-8 (4)
ADRELVHMINWAKRVPGFVDL	350	370	3	-5 (4)*	-10 (3)	-7 (3)	-8 (4)
LVHMINW	354	360	2	-3 (3)*	-10 (3)	-11 (3)	-7 (3)
VDLTLHD	368	374	2	4 (6)*	-7 (5)	-6 (4)	-2 (6)*
VDLTLHDQVHLLE	368	380	3	4 (5)*	-5 (3)	-5 (2)*	-6 (4)
LTLHDQVHLLE	370	380	2	4 (4)*	-4 (2)*	-3 (2)*	-4 (3)*
HDQVHLLE	373	380	2	2 (4)*	-4 (1)*	-4 (2)*	-4 (3)*
LVWRSMEHPGKL	391	402	3	-6 (5)	-7 (4)	-6 (3)	-7 (4)
LVWRSMEHPGKLLF	391	404	3	-7 (5)	-8 (4)	-8 (4)	-8 (4)
LVWRSMEHPGKLLFAPNLL	391	409	3	-9 (6)	-11 (4)	-8 (5)	-10 (5)
VWRSMEHPGKL	392	402	3	-6 (5)	-7 (4)	-7 (3)	-7 (3)
VWRSMEHPGKLLFAPNLLL	392	410	3	-9 (6)	-11 (4)	-8 (5)	-10 (4)
LFAPNL	403	408	1	-13 (7)	-20 (6)	-16 (5)	-17 (5)
LFAPNLLL	403	410	2	-10 (6)	-15 (6)	-13 (5)	-14 (7)
LLDRNQGKCVEG	409	420	2	-9 (7)	-15 (5)	-1 (6)*	0 (8)*
LLDRNQGKCVEGMVE	409	423	3	-8 (6)	-13 (6)	-1 (6)*	0 (7)*
LDRNQGKCVEG	410	420	2	-9 (8)	-16 (7)	-4 (4)*	0 (9)*
MVEIF	421	425	1	-7 (3)	-9 (2)	-6 (2)	4 (4)*
MVEIFDML	421	428	1	-10 (5)	-13 (4)	-7 (5)	6 (8)
VEIFDML	422	428	1	-12 (3)	-18 (4)	-9 (5)	7 (6)
LATSSRF	429	435	2	-5 (9)*	-6 (5)	-2 (4)*	-9 (9)
LATSSRFRM	429	437	2	-4 (7)*	-5 (3)*	-2 (3)*	-8 (7)
LATSSRFRMMNLQGEEF	429	445	3	-3 (5)*	-3 (3)*	-2 (3)*	-6 (6)
ATSSRFRMMNLQGEE	430	444	3	-3 (6)*	-5 (4)	-1 (3)*	-7 (7)
RMMNLQGEEF	436	445	2	-3 (6)*	-4 (3)*	-2 (4)*	-7 (8)
KSIIL	449	453	1	-1 (2)*	-2 (2)*	0 (1)*	-3 (4)*
LNSGVYTFL	454	462	1	2 (5)*	-1 (5)*	0 (5)*	3 (7)*
TFLSSTL	460	466	1	2 (3)*	1 (5)*	2 (4)*	4 (10)*
SSTLKSLEEKDHIHRVLDKITDTL	463	486	3	1 (3)*	-1 (3)*	0 (2)*	0 (4)*
KSLEEKDHIHRVLDKITDTL	467	486	3	1 (4)*	0 (5)*	1 (3)*	-2 (3)*
IHLMAKAGLTLQQQHQRLAQL	487	507	3	2 (4)*	1 (4)*	3 (2)*	-1 (3)*
LLILSHIRHMSNKGMEHL	508	525	3	-10 (4)	-12 (2)	-10 (2)	-9 (9)
LILSHIRHMSNKGMEHL	509	525	2	-11 (4)	-12 (3)	-10 (2)	-8 (9)
LILSHIRHMSNKGMEHL	509	525	4	-11 (4)	-13 (3)	-11 (3)	-9 (9)
ILSHIRHMSNKGMEHL	510	525	3	-12 (4)	-13 (3)	-12 (3)	-10 (10)
YSMKCKNVVPLSDLL	526	540	2	-7 (7)	-18 (8)	-8 (5)	8 (7)
YSMKCKNVVPLSDLL	526	540	3	-7 (7)	-19 (7)	-8 (4)	8 (9)
LLEML	540	544	1	-5 (6)	-22 (5)	-23 (3)	3 (9)*
LEMLDA	541	546	1	-21 (10)	-43 (6)	-35 (6)	7 (9)
EMLDAHRLHAPTS	542	554	2	-4 (6)*	-9 (5)	-6 (4)	3 (8)*
DAHRLHAPTS	545	554	2	1 (4)*	-1 (5)*	1 (4)*	3 (7)*
HRLHAPTS	547	554	2	2 (4)*	0 (5)*	1 (4)*	1 (8)*

Figure 7—figure supplement 5. Experiment comparison view comparing the differential HDX behavior of *apo* Y537S ERα LBD in the presence of various ligands or coactivator.

DOI: https://doi.org/10.7554/eLife.12792.033

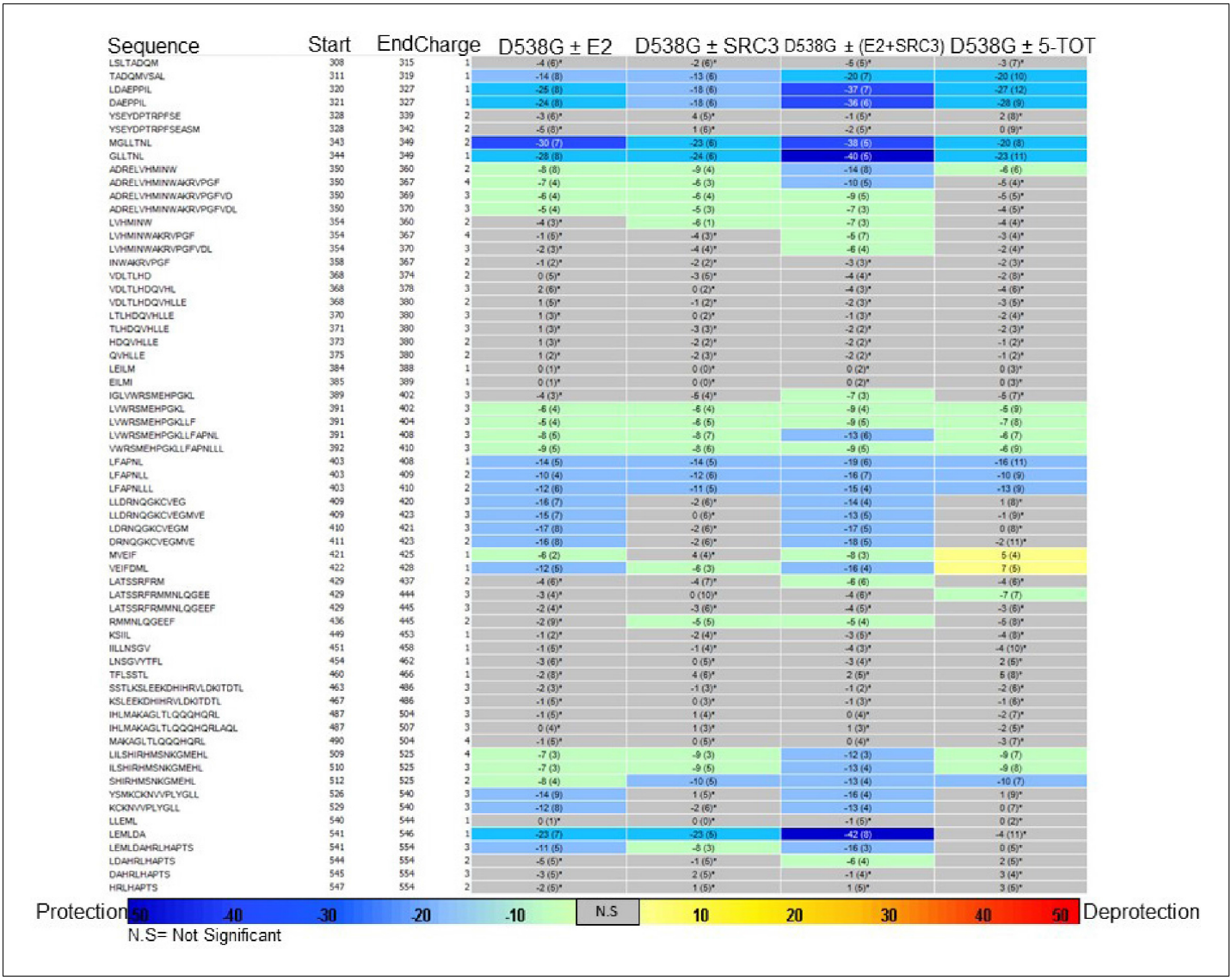

Sequence	Start	End	Charge	D538G ± E2	D538G ± SRC3	D538G ± (E2+SRC3)	D538G ± 5-TOT
LSLTADQM	308	315	1	-4 (6)*	-2 (6)*	-5 (5)*	-3 (7)*
TADQMVSAL	311	319	1	-14 (8)	-13 (6)	-20 (7)	-20 (10)
LDAEPPIL	320	327	1	-25 (8)	-18 (6)	-37 (7)	-27 (12)
DAEPPIL	321	327	1	-24 (8)	-18 (6)	-36 (6)	-28 (9)
YSEYDPTRPFSE	328	339	2	-3 (6)*	4 (5)*	-1 (5)*	2 (8)*
YSEYDPTRPFSEASM	328	342	2	-5 (6)*	1 (6)*	-2 (5)*	0 (9)*
MGLLTNL	343	349	2	-30 (7)	-23 (6)	-38 (5)	-20 (8)
GLLTNL	344	349	1	-28 (8)	-24 (6)	-40 (5)	-23 (11)
ADRELVHMINW	350	360	2	-8 (8)	-9 (4)	-14 (8)	-6 (6)
ADRELVHMINWAKRVPGF	350	367	4	-7 (4)	-6 (3)	-10 (5)	-5 (4)*
ADRELVHMINWAKRVPGFVD	350	369	3	-6 (4)	-6 (4)	-9 (5)	-5 (5)*
ADRELVHMINWAKRVPGFVDL	350	370	3	-5 (4)	-5 (3)	-7 (3)	-4 (5)*
LVHMINW	354	360	2	-4 (3)*	-6 (1)	-7 (3)	-4 (4)*
LVHMINWAKRVPGF	354	367	4	-1 (5)*	-4 (3)*	-5 (7)	-3 (4)*
LVHMINWAKRVPGFVDL	354	370	3	-2 (3)*	-4 (4)*	-6 (4)	-2 (4)*
INWAKRVPGF	358	367	2	-1 (2)*	-2 (2)*	-3 (3)*	-2 (3)*
VDLTLHD	368	374	2	0 (5)*	-3 (5)*	-4 (4)*	-2 (8)*
VDLTLHDQVHL	368	378	3	2 (6)*	0 (2)*	-4 (3)*	-4 (6)*
VDLTLHDQVHLLE	368	380	2	1 (5)*	-1 (2)*	-2 (3)*	-3 (5)*
LTLHDQVHLLE	370	380	3	1 (3)*	0 (2)*	-1 (3)*	-2 (4)*
TLHDQVHLLE	371	380	3	1 (3)*	-3 (3)*	-2 (2)*	-2 (3)*
HDQVHLLE	373	380	2	1 (3)*	-2 (2)*	-2 (2)*	-1 (2)*
QVHLLE	375	380	2	1 (2)*	-2 (3)*	-2 (2)*	-1 (2)*
LEILM	384	388	1	0 (1)*	0 (0)*	0 (2)*	0 (3)*
EILMI	385	389	1	0 (1)*	0 (0)*	0 (2)*	0 (3)*
IGLVWRSMEHPGKL	389	402	3	-4 (3)*	-5 (4)*	-7 (3)	-5 (7)*
LVWRSMEHPGKL	391	402	3	-6 (4)	-5 (4)	-9 (4)	-5 (9)
LVWRSMEHPGKLLF	391	404	3	-5 (4)	-6 (5)	-9 (5)	-7 (8)
LVWRSMEHPGKLLFAPNL	391	408	3	-8 (5)	-8 (7)	-13 (6)	-6 (7)
VWRSMEHPGKLLFAPNLLL	392	410	3	-9 (5)	-8 (6)	-9 (5)	-6 (9)
LFAPNL	403	408	1	-14 (5)	-14 (5)	-19 (6)	-16 (11)
LFAPNLL	403	409	2	-10 (4)	-12 (6)	-16 (7)	-10 (9)
LFAPNLLL	403	410	2	-12 (6)	-11 (5)	-15 (4)	-13 (9)
LLDRNQGKCVEG	409	420	3	-16 (7)	-2 (6)*	-14 (4)	1 (8)*
LLDRNQGKCVEGMVE	409	423	3	-15 (7)	0 (6)*	-13 (5)	-1 (9)*
LDRNQGKCVEGM	410	421	3	-17 (8)	-2 (6)*	-17 (5)	0 (8)*
DRNQGKCVEGMVE	411	423	2	-16 (8)	-2 (6)*	-18 (5)	-2 (11)*
MVEIF	421	425	1	-6 (2)	4 (4)*	-8 (3)	5 (4)
VEIFDML	422	428	1	-12 (5)	-6 (3)	-16 (4)	7 (5)
LATSSRFRM	429	437	2	-4 (6)*	-4 (7)*	-6 (6)	-4 (6)*
LATSSRFRMMNLQGEE	429	444	3	-3 (4)*	0 (10)*	-4 (6)*	-7 (7)
LATSSRFRMMNLQGEEF	429	445	3	-2 (4)*	-3 (6)*	-4 (5)*	-3 (6)*
RMMNLQGEEF	436	445	2	-2 (9)*	-5 (5)	-5 (4)	-5 (8)*
KSIIL	449	453	1	-1 (2)*	-2 (4)*	-3 (5)*	-4 (8)*
IILLNSGV	451	458	1	-1 (5)*	-1 (4)*	-4 (3)*	-4 (10)*
LNSGVYTFL	454	462	1	-3 (6)*	0 (5)*	-3 (4)*	2 (5)*
TFLSSTL	460	466	1	-2 (8)*	4 (6)*	2 (5)*	5 (8)*
SSTLKSLEEKDHIHRVLDKITDTL	463	486	3	-2 (3)*	-1 (3)*	-1 (2)*	-2 (6)*
KSLEEKDHIHRVLDKITDTL	467	486	3	-1 (5)*	0 (3)*	-1 (3)*	-1 (6)*
IHLMAKAGLTLQQQHQRL	487	504	3	-1 (5)*	1 (4)*	0 (4)*	-2 (7)*
IHLMAKAGLTLQQQHQRLAQL	487	507	3	0 (4)*	1 (3)*	1 (3)*	-2 (5)*
MAKAGLTLQQQHQRL	490	504	4	-1 (5)*	0 (5)*	0 (4)*	-3 (7)*
LILSHIRHMSNKGMEHL	509	525	4	-7 (3)	-9 (3)	-12 (3)	-9 (7)
ILSHIRHMSNKGMEHL	510	525	3	-7 (3)	-9 (5)	-13 (4)	-9 (8)
SHIRHMSNKGMEHL	512	525	2	-8 (4)	-10 (5)	-13 (4)	-10 (7)
YSMKCKNVVPLYGLL	526	540	3	-14 (9)	1 (5)*	-16 (4)	1 (9)*
KCKNVVPLYGLL	529	540	3	-12 (8)	-2 (6)*	-13 (4)	0 (7)*
LLEML	540	544	1	0 (1)*	0 (0)*	-1 (5)*	0 (2)*
LEMLDA	541	546	1	-23 (7)	-23 (5)	-42 (8)	-4 (11)*
LEMLDAHRLHAPTS	541	554	3	-11 (5)	-8 (3)	-16 (3)	0 (5)*
LDAHRLHAPTS	544	554	2	-5 (5)*	-1 (5)*	-6 (4)	2 (5)*
DAHRLHAPTS	545	554	3	-3 (5)*	2 (5)*	-1 (4)*	3 (4)*
HRLHAPTS	547	554	2	-2 (5)*	1 (5)*	1 (5)*	3 (5)*

Figure 7—figure supplement 6. Experiment comparison view comparing the differential HDX behavior of *apo* D538G ERα LBD in the presence of various ligands or coactivator.

DOI: https://doi.org/10.7554/eLife.12792.034

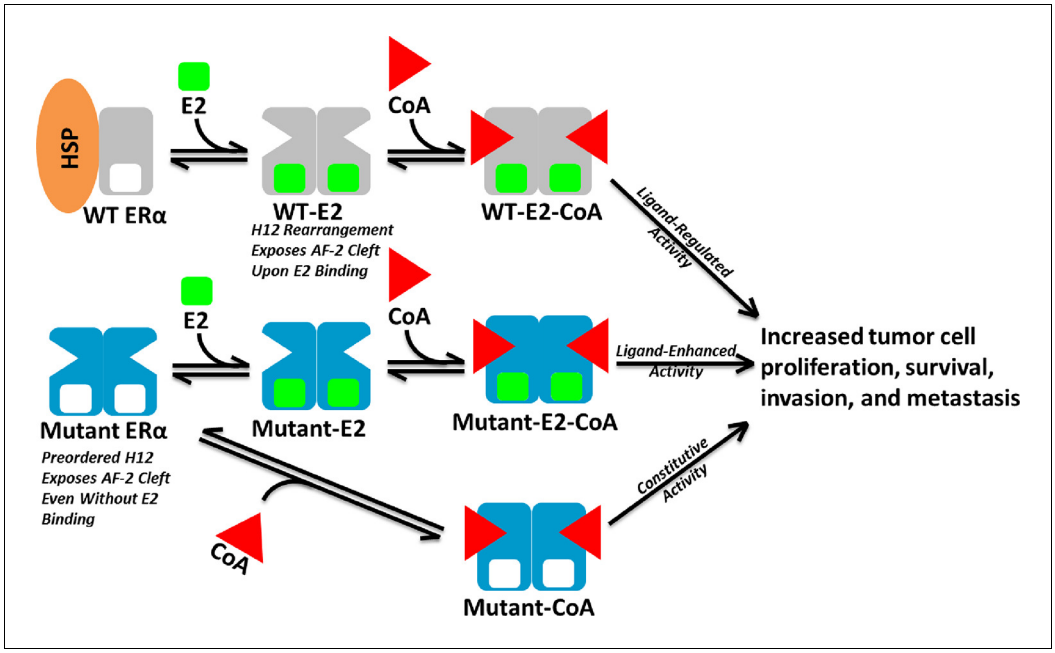

Figure 8. Model of Aberrent ERα Mutant Activity. Upon hormone binding (E2), WT ERα sheds heat-shock/chaperone proteins (HSP), forms head-to-head homodimers, and recruits coactivator (CoA) to become active. By contrast, Y537S or D538G ERα mutants adopt the active conformation in the absence of hormone to recruit CoA and achieve constitutive activity. Additionally, E2 binding may further increase mutant activity.
DOI: https://doi.org/10.7554/eLife.12792.035